Received: 21 April 2023 | Revised: 18 September 2023 | Accepted: 15 October 2023

DOI: 10.1002/pro.4809

RESEARCH ARTICLE

THE PROTEIN SOCIETY WILEY

Revisiting the hydrolysis of ampicillin catalyzed by Temoneira-1 β-lactamase, and the effect of Ni(II), Cd(II) and Hg(II)

Zeyad H. Nafaee[1,2] | **Viktória Egyed**[1] | **Attila Jancsó**[1] | **Annamária Tóth**[1] | **Adeleh Mokhles Gerami**[3,4] | **Thanh Thien Dang**[5] | **Juliana Heiniger-Schell**[4,5] | **Lars Hemmingsen**[6] | **Éva Hunyadi-Gulyás**[7] | **Gábor Peintler**[8] | **Béla Gyurcsik**[1]

[1]Department of Molecular and Analytical Chemistry, University of Szeged, Szeged, Hungary

[2]College of Pharmacy, University of Babylon, Babel, Iraq

[3]School of Particles and Accelerators, Institute for Research in Fundamental Sciences (IPM), Tehran, Iran

[4]European Organization for Nuclear Research (CERN), Geneva, Switzerland

[5]Institute for Materials Science and Center for Nanointegration Duisburg-Essen (CENIDE), University of Duisburg-Essen, Essen, Germany

[6]Department of Chemistry, University of Copenhagen, Copenhagen, Denmark

[7]Laboratory of Proteomics Research, Biological Research Centre, Hungarian Research Network (HUN-REN), Szeged, Hungary

[8]Department of Physical Chemistry and Material Sciences, University of Szeged, Szeged, Hungary

Correspondence
Béla Gyurcsik, Department of Inorganic, Organic and Analytical Chemistry, University of Szeged, Dóm tér 7, H-6720 Szeged, Hungary.
Email: gyurcsik@chem.u-szeged.hu

Funding information
FCT-Portugal, Grant/Award Number: CERN-FIS-PAR-0005-2017; EURONS; European Union's Horizon 2020 Framework, Grant/Award Numbers: 101057511 (EURO-LABS), 654002 (ENSAR2); Federal Ministry of Education and Research, Grant/Award Numbers: 05K16PGA, 05K22PGA; Nemzeti Kutatási Fejlesztési és Innovációs Hivatal, Grant/Award Number: GINOP-2.3.2-15-2016-00038; NICE; Hungarian National Research, Development and Innovation Office, Grant/Award Numbers: 2019-2.1111-TÉT-2019-00089, GINOP-2.3.2-15-2016-00020, GINOP-2.3.2-15-2016-00001, GINOP-2.3.2-15-2016-00038

Abstract

β-Lactamases grant resistance to bacteria against β-lactam antibiotics. The active center of TEM-1 β-lactamase accommodates a Ser-Xaa-Xaa-Lys motif. TEM-1 β-lactamase is not a metalloenzyme but it possesses several putative metal ion binding sites. The sites composed of His residue pairs chelate borderline transition metal ions such as Ni(II). In addition, there are many sulfur-containing donor groups that can coordinate soft metal ions such as Hg(II). Cd(II) may bind to both types of the above listed donor groups. No significant change was observed in the circular dichroism spectra of TEM-1 β-lactamase on increasing the metal ion content of the samples, with the exception of Hg(II) inducing a small change in the secondary structure of the protein. A weak nonspecific binding of Hg(II) was proven by mass spectrometry and ^{119m}Hg perturbed angular correlation spectroscopy. The hydrolytic process of ampicillin catalyzed by TEM-1 β-lactamase was described by the kinetic analysis of the set of full catalytic progress curves, where the slow, yet observable conversion of the primary reaction product into a second one, identified as ampilloic acid by mass spectrometry, needed also to be considered in the applied model. Ni(II) and Cd(II) slightly promoted the catalytic activity of the enzyme while Hg(II) exerted a noticeable inhibitory effect. Hg(II) and Ni(II),

Review Editor: Aitziber L. Cortajarena

applied at 10 μM concentration, inhibited the growth of *E. coli* BL21(DE3) in M9 minimal medium in the absence of ampicillin, but addition of the antibiotic could neutralize this toxic effect by complexing the metal ions.

KEYWORDS

^{199m}Hg perturbed angular correlation spectroscopy of γ-rays, circular dichroism, mass spectrometry, reaction kinetics, TEM-1 β-lactamase, toxic metal binding

1 | INTRODUCTION

β-Lactamases hydrolyze the β-lactam ring of antibiotics before they can interact with bacterial carboxy-transpeptidases, providing thereby resistance toward β-lactam antibiotics (Oka et al., 1980). Based on their catalytic mechanism, the four classes of β-lactamases are termed A, B, C, and D. The active sites of classes A, C, and D, called also serine β-lactamases, contain a Ser-Xaa-Xaa-Lys (SXXK) motif. Class B is a heterogeneous group of Zn(II) metalloenzymes called metallo-β-lactamases. The SXXK motif employs Ser as a nucleophile hydrolyzing β-lactams by forming covalent acylenzyme intermediate, while metallo-β-lactamases utilize a Zn(II)-activated water molecule as a nucleophile (Bush et al., 1995; Bush and Jacoby, 2010; Nagshetty et al., 2021; Massova and Mobashery, 1998; Matagne et al., 1998; Naas et al., 2017). All serine β-lactamases employ an acylation–deacylation mechanism. The nucleophilic Ser is activated by a general base, then it attacks the carbonyl carbon atom of the β-lactam amide bond and generates the acylenzyme intermediate (tetrahedral oxyanion transition state). Finally, a water molecule is activated by a general base to hydrolyze the acylenzyme adduct. Still there is a debate about the identity of the general base activating the serine residue. Both Lys (part of the SXXK motif) and the deprotonated sidechain of a Glu close to the active center have been proposed to fulfill this function, and both mechanisms were supported by crystallographic studies of enzyme complexes, computational simulations, and biochemical investigations of enzyme mutants (Matagne and Frère, 1995; Strynadka et al., 1992; Damblon et al., 1996; Tooke et al., 2019; Egorov et al., 2019; Wang et al., 2003; Minasov et al., 2002).

TEM-1 β-lactamase is a well-known representative of the extended spectrum serine β-lactamases. Its gene is incorporated into various DNA vectors as a selectable marker in biochemistry research. As a source of development of bacterial antibiotic resistance, TEM-1 β-lactamase and its mutants are frequent targets of the scientific research (Cumming et al., 2022; Birgy et al., 2022; Palzkill, 2018; Madzgalla et al., 2021; Bratulic et al., 2015; Wuerz et al., 2020; Zimmerman et al., 2017; Dellus-Gur et al., 2015). TEM-1 β-lactamases, isolated from various bacteria, display few differences in their amino acid sequences. Over 170 natural and even more 'in vitro' catalytically active mutants were reported (Salverda et al., 2010; Jacquier et al., 2013; Kather et al., 2008). The kinetic parameters for the TEM-1 β-lactamase catalyzed hydrolysis of ampicillin as a substrate were determined earlier to evaluate their catalytic performance of this enzyme (Table 1). k_{cat} values were in the range of 800–2000 s^{-1} while the Michaelis–Menten constants (K_M) varied between 20 and 77 μM.

TEM-1 β-lactamase is not a metalloenzyme, but its available structures suggest possible metal binding spots in the sidechains of six histidine, two cysteine, and nine methionine residues (Scheme 1). The crystal structure of a TEM-1 β-lactamase (Stec et al., 2005) with a sequence differing only in a single amino acid (V82I mutation according to the standard numbering of class A β-lactamases (Ambler et al., 1991) from the presently studied enzyme indicated three putative metal ion binding sites for borderline transition metal ions on the protein surface, each composed of two His residues. These sites have previously been shown to be useful for purification by Ni(II)- or Zn(II)-affinity chromatography without introducing any artificial purification tag (Nafaee et al., 2023; Lawung et al., 2001; Yang et al., 2020). Although Hg(II) can bind to favorable His sites, but in general, its affinity toward the imidazole nitrogen is low (Stratton et al., 2017). The 2.0 Å distance between the sulfur atoms of the two Cys residues suggested that these sidechains are involved in a structural disulfide bridge (Sun et al., 2017) that is rarely bound to metal ions. Nevertheless, metal ions of soft Lewis acid character, such as Hg(II) were shown to interact with a disulfide bridge (Brown and Edwards, 1969). Similarly, the sulfur donor atoms of the thioether groups were shown to be able to bind Hg(II) and more weakly Cd(II) and Ni(II) in various amino acids, peptides and proteins (Birgersson et al., 1973; Lenz and Martell, 1964; Sóvágó and Petőcz, 1987; Latha et al., 2007). In the crystal structure of the Hg(II) bismethioninato complex the interaction occurs through two thioether–mercury bonds with the Hg–S distances of 2.5 Å (Carty and Taylor, 1976).

TABLE 1 k_{cat} and K_M values of TEM-1 β-lactamase using ampicillin as a substrate.

k_{cat} (s^{-1})	K_M (μM)	k_{cat}/K_M ($\mu M^{-1} s^{-1}$)	Medium	Temp. (°C)	Reference
1428 ± 24	50 ± 2	28.6 ± 5.5	50 mM phosphate buffer (pH 7.0)	30	Cantu et al. (1997)
1460	60	24	50 mM phosphate buffer (pH 7.0)	37	Lawung et al. (2001)
1085 ± 137	38 ± 18	29	50 mM phosphate buffer (pH 7.0)	30	Brown et al. (2009)
1653 ± 370	63 ± 14	26	50 mM phosphate buffer (pH 7.2)	30	Stojanoski et al. (2015)
830 ± 30	58 ± 1	14	50 mM phosphate buffer (pH 7.0)	30	Sideraki et al. (2001)
1428	50	28.58	50 mM phosphate buffer (pH 7.0)	30	Stiffler et al. (2015)
960	65.2	14.8	50 mM phosphate buffer (pH 7.0); 1 mg/mL BSA	30	Marciano et al. (2009)

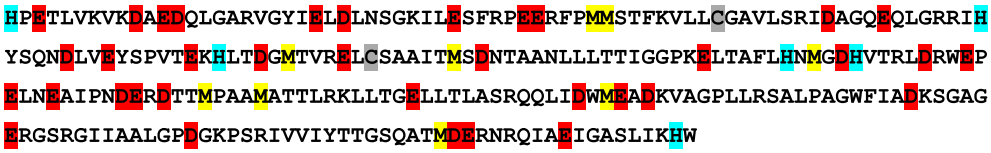

SCHEME 1 The amino acid sequence of the studied mature TEM-1 β-lactamase. The amino acids containing potential donor groups for metal ion coordination are highlighted by background colors: His—blue, Cys—gray, Met—yellow and the negatively charged Asp and Glu by red.

However, the apparent binding affinity for a monodentate thioether coordination to Hg(II), determined only in ternary complexes, is in the order of $\sim 10^5\ M^{-1}$ (Pyreu et al., 2011). Comparable K_d values were obtained for the methionine sidechain coordination to Cu(I)—a soft metal ion similar to Hg(II)—in various peptide models of the Ctr1 copper transport protein, ranging between 2 and 10 μM (Rubino et al., 2010). Methionine based turn-on sensors have been successfully applied for the selective detection of Hg(II) (Scully et al., 2008; Yang et al., 2011). Furthermore, Delangle and coworkers showed for Cu(I) that with a preorganized binding site consisting of methionines, the metal binding affinity can be increased by several orders of magnitude (Jullien et al., 2015).

In addition to the above listed primary N and S donor atoms, the presence of nearby carboxylic groups of aspartic and glutamic acid units, carboxamide groups of asparagine and glutamine residues, as well as hydroxy groups of serine and threonine residues may increase the binding affinity of metal ions by offering further O donor atoms for coordination (Fragoso et al., 2013; Miller et al., 2018; Potocki et al., 2019; Remelli et al., 2018).

Based on the above findings our hypothesis is that metal ions may influence the structure and catalytic activity of TEM-1 β-lactamase. Therefore, the aim of this research was to assess the catalytic activity of the enzyme in the absence and presence of metal ions against ampicillin substrate by spectrophotometry. The effect of metal ions on the growth of bacterial cultures in M9 minimal medium (Miller, 1972) was also monitored. In line with the catalytic properties, we verified the interaction of Hg(II) with TEM-1 β-lactamase by circular dichroism (CD) and ^{199m}Hg perturbed angular correlation of γ-rays (PAC) spectroscopy as well as mass spectrometry (MS).

2 | RESULTS AND DISCUSSION

2.1 | Hydrolysis of ampicillin and the catalytic activity of TEM-1 β-lactamase

The sequence of the mature TEM-1 β-lactamase applied in our experiments is depicted in Scheme 1. This enzyme is encoded by the pET-21a DNA vector and serves to provide antibiotic resistance to transformed bacteria against ampicillin. This enzyme is not a metalloenzyme but offers a large number of donor groups which can interact with various kinds of metal ions. Prior to reveal the effect of metal ions on the enzyme activity, we quantitatively investigated the catalytic activity of the purified TEM-1 β-lactamase using ampicillin as a substrate.

The efficiency of TEM-1 β-lactamase is often characterized by the specific activity. The units for specific activity are defined as millimoles ampicillin hydrolyzed per minute per mg total protein or mg of protein, but the unit of enzyme activity may be defined in a different way/more precisely as the amount of enzyme that hydrolyzes 1 μmol of substrate in 1 min at 30°C in 0.05 M phosphate buffer (pH 7.0) (Huang et al., 1996; Huang and Palzkill, 1997; Minami et al., 1980). Because of the

use of varying definitions and conditions (buffer, pH, temperature) as well as various substrates and TEM-1 β-lactamase sequence deviations from different bacteria, it is difficult to appropriately compare the available data. For ampicillin, the absorbance values collected at 235 nm are generally accepted in the literature by considering this wavelength optimal to follow the hydrolytic process. The difference in the molar absorbances of the substrate and the product was previously determined to be between 670 and 900 M^{-1} cm^{-1}, with the molar absorbance of the substrate falling in between 1710 and 2160 M^{-1} cm^{-1} (Table 2) (Waley, 1974; Samuni, 1975; Minami et al., 1980; Huang and Palzkill, 1997). Molar absorbance values of ampicillin (1921 M^{-1} cm^{-1}) and the hydrolysis product (1041 M^{-1} cm^{-1}) determined previously in our laboratory were within the reported ranges, and the average specific activity was 596 ± 25 μmol of ampicillin hydrolyzed by 1 mg of TEM-1 β-lactamase within 1 min at 25°C in 20 mM Tris–HCl (pH 7.5) (Nafaee et al., 2023).

There are significantly more publications in the literature evaluating the catalytic experiments through the V_{max} and/or k_{cat} and K_M parameters (often k_{cat}/K_M values are used to characterize the enzyme efficiency) instead of the specific activity. These parameters are determined by the initial rate kinetic analysis using the Michaelis–Menten formalism. The data collected in Table 1 cannot be considered fully independent, since most of them were determined by the same research group (Cantu et al., 1997; Brown et al., 2009; Stojanoski et al., 2015; Sideraki et al., 2001; Marciano et al., 2009). In spite of this, relatively large deviations were observed for different batches of the enzyme. It is also noticeable that different DNA plasmids (i.e., potentially slightly different TEM-1 β-lactamase sequences), and partially different conditions were applied in these studies (see Table 1). Nevertheless, using the Michaelis–Menten formalism to treat the data, providing the k_{cat} and K_M or the k_{cat}/K_M values as kinetic parameters characterizing the enzymatic reaction is still a common procedure (Song and Tezcan, 2014; Bahr et al., 2021; Judge et al., 2023) most probably due to their comparability.

In the first series of our measurements in 20 mM Tris–HCl (pH 7.5) buffer at 25°C, the nominal substrate concentration was either 230 or 930 μM while the enzyme concentration ranged between 0.2 and 1.2 nM (Series 1). The hydrolytic process of the substrate was followed spectrophotometrically in the 210–235 nm wavelength range instead of using a single wavelength, allowing to collect an informative set of absorbance data. The linear relationship between the concentrations and the measured absorbances was strictly valid in the 0–2.5 absorbance range. Therefore, the measured data above the value of $A = 2.5$ were ignored during the evaluation. Fast conversion of the substrate was observed (see Figure 2 below) however, a slow but continuous decrease of the measured values was experienced upon recording the absorbances for an extended period. This suggested a further transformation of the primary reaction product, which may affect the mathematical treatment of the data, that is, the kinetic model. Previous studies on the degradation processes of ampicillin and similar antibiotics revealed that the primary hydrolysis product may be converted into different molecules depending on the pH and temperature (Mitchell et al., 2014; Sy et al., 2017; Raza Siddiqui et al., 2014; Robinson-Fuentes et al., 1997; Nägele and Moritz, 2005). This phenomenon may also account for the ambiguity in the determination of the molar absorbance of the hydrolysis product (Table 2). These findings inspired us to apply the matrix rank analysis on the recorded absorbance data set (Peintler et al., 1997) to conclude the number of independent absorbing species (NIAS) needed for description of the catalytic system. The main advantage of this method is that the determined NIAS is independent of both the specific chemical model and the concentration uncertainties. The inspection of the so called "residual absorbance curves", that is, the unexplained absorbances upon

TABLE 2 The molar absorbance values at 235 nm (ε_{235nm}) for ampicillin and the hydrolysis product, as well as their differences collected from the literature.

ε_{235nm} (Amp) (M^{-1} cm^{-1})	$\Delta\varepsilon$ (A–P)$_{235nm}$ (M^{-1} cm^{-1})	ε_{235nm} (product) (M^{-1} cm^{-1})	Reference
1710	670	1040 (calc)	Waley (1974)
-	820	-	Samuni (1975) and Citri et al. (1976)
-	900	-	Minami et al. (1980)
2160	900	1260 (calc)	Huang and Palzkill (1997)
-	820	-	Lund et al. (2016)
1921	880	1041	Nafaee et al. (2023)

Note: The ε_{235nm} (product) values were calculated from the published data, whenever these were provided.

increasing the supposed number of colored species clearly revealed that after including two species (e.g., the substrate and the hydrolysis product), there is still a systematic and significant deviation from the noise (a few milliabsorbances) of the spectrophotometric experiment (Figure 1). Considering a third colored species, these systematic deviations disappeared. These results necessitated the inclusion of a second product in the mathematical treatment of the data. To our knowledge, the formation of the second product was not considered in TEM-1 β-lactamase-catalyzed ampicillin hydrolysis studies so far.

All the data collected in the Series 1 experiments were treated together in the full kinetic description of the system by assuming the presence of a second product. The stoichiometric and rate equations of the model applied in the calculations consisted of the following steps:

$$\begin{aligned} S + E &\underset{k_2}{\overset{k_1}{\rightleftharpoons}} (ES) && , r_1 = k_1 \cdot [S] \cdot [E] \text{ and } r_2 = k_2 \cdot [(ES)] \\ (ES) &\xrightarrow{k_3} P_1 + E && , r_3 = k_3 \cdot [(ES)] \\ P_1 &\xrightarrow{k_4} P_2 && , r_4 = k_4 \cdot [P_1] \end{aligned} \quad (1)$$

where S denotes the substrate, E stands for the enzyme, (ES) is the enzyme–substrate complex as a macroscopic species including all possible microscopic species, P_1 and P_2 are the initial and the secondary products, respectively and r_i is the reaction rate of the ith step. As it is shown in Figure 2 and S1, the curves could be fitted well with this model, unlike with the simpler model excluding the second product (P_2). As expected, the latter model cannot appropriately describe well especially those parts of the experimental curves, where the conversion of P_1 into P_2 dominates.

The kinetic experiments executed with different starting concentrations of the substrate and the enzyme, clearly revealed that the partial adjustment of the initial enzyme concentrations is necessary for the proper fit of the curves. This indicated that the enzyme is very sensitive to any change of the conditions during its treatment, for example, the freeze/thaw procedure, composition of the storage buffer, extreme dilution and temperature change. The experimental errors arising from the pipetting of volumes in the few μL range, the material of the pipette tips and sample containers causing eventual adsorption of the enzyme also influenced the obtained experimental data. However, the simultaneous evaluation of all the catalytic experiments performed in the same buffer and temperature

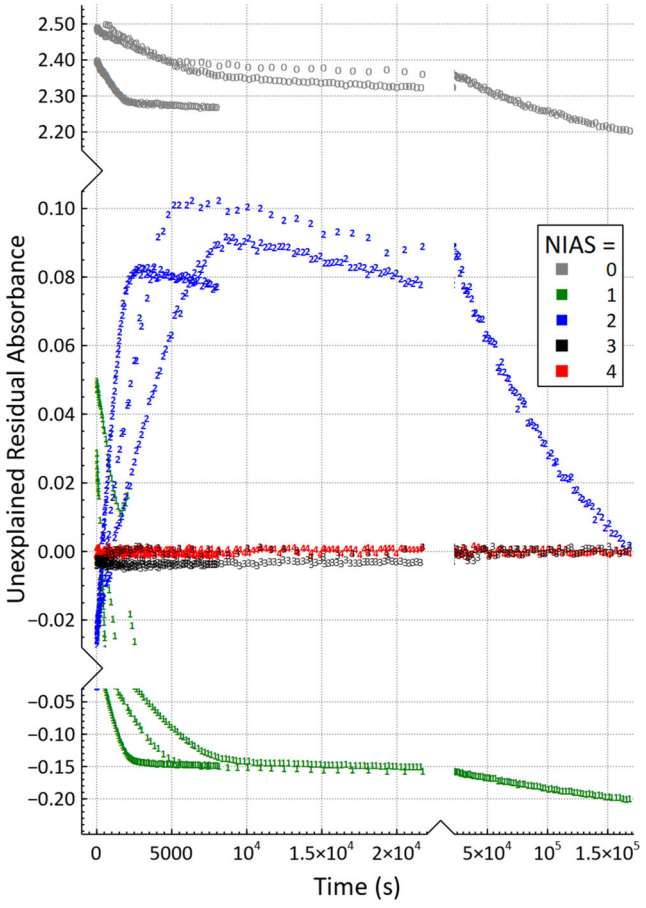

FIGURE 1 The residual absorbance curves calculated using matrix rank analysis to determine the minimal number of spectrally independent absorbing species (NIAS). The data used for this calculation were all recorded absorbances at the lower initial substrate concentration (~230 μM) in the 235–214 nm range of Series 1 kinetic experiments. The systematic deviation of the residual absorbances from the noise level upon sequential inclusion of new colored species indicated the presence of at least three absorbing species.

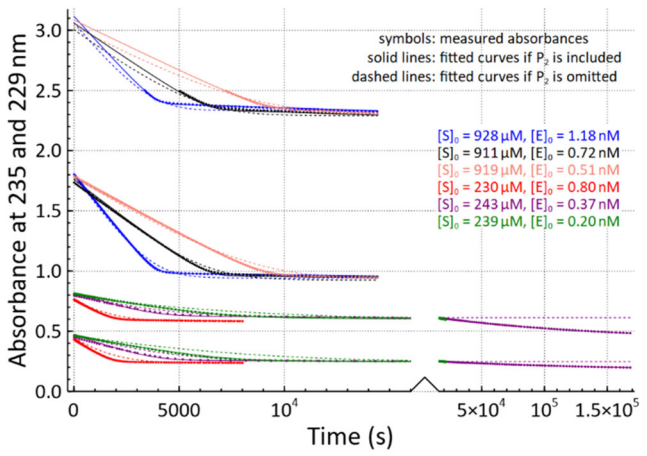

FIGURE 2 TEM-1 β-lactamase activity monitored by spectrophotometry via the hydrolysis of ampicillin as a substrate in the Series 1 experiments. Only absorbances obtained at 235 and 229 nm are shown in the figure, while the results of the calculations at all applied wavelength values are included in Figure S1.

conditions yielded a single parameter set with a good agreement between the fitted and experimental data. Thus, the enzyme performance in the catalytic process could be unambiguously characterized.

The kinetic data, as well as the spectral parameters of the species obtained from this evaluation are included in Table 3. The determined fairly low k_3 value can be attributed to the applied measurement conditions. Therefore, we have repeated the kinetic experiments also under the most frequently applied conditions reported in the literature: 50 mM phosphate (pH 7.0) buffer at 30°C. The evaluation of these experiments (Series 2) yielded parameters comparable to those previously published (Tables 1 and 3) but complementing the results with information about the second hydrolytic product. It is notable that the increase of the temperature in the second series by just 5°C significantly increased the yield of P_2 as compared to Series 1 executed at 25°C. This is also an indication that the transformation of the primary product P_1 clearly needs to be taken into account in the characterization of the ampicillin hydrolysis.

The k_4 value, characteristic for the conversion of P_1 into P_2, is very small however, the concentration of P_1 is higher than the enzyme concentration by several orders of magnitude. Therefore, P_2 is formed in significant amounts as shown in the species distribution in the time course of the hydrolysis (Figure 3). The chemical reactions are going on practically three different time scales. The formation of the enzyme-substrate complex is completed within a few milliseconds. However, not all enzyme is transformed to complex since the rate of the first step (belonging to k_1) is continuously decreasing while the rate of P_1 formation (related to k_3) is increasing during this first stage of the reaction. At about three milliseconds, the rates of these two steps become comparable and the decomposition of the complex continuously retrieving the free enzyme. We shall mention, that this part of the curves in Figure 3 is extrapolated, since our experiments do not contain data within this short time interval. Recent time-resolved X-ray diffraction data demonstrated changes in the millisecond interval of the hydrolytic reaction catalyzed by a metallo-β-lactamase, proving that the ES complex itself is a macroscopic species being transformed in several steps before the product formation (Wilamowski et al., 2022). Similar studies with serine-β-lactamases may provide deep insight into the mechanism of action and are very welcome in the future. Fast kinetic methods such as the flow and relaxation methods may also contribute to determine further rate constants even in complicated branched catalytic pathways of -β-lactam hydrolysis (Punekar, 2018; Galleni and Frère, 2007). Such studies under single turnover kinetic conditions allowed for determination of the rate of the covalent enzyme–substrate complex formation, and/or of its decomposition rate constant (Furey et al., 2021; Mehta et al., 2021). The latter rate constants are not independent as they can be derived from each other by using the appropriate formula and knowing the k_{cat} value.

In the second timescale (up to ~4 h), almost the full amount of the substrate disappears, and the main reaction of the last stage is the formation of P_2 from P_1. The figure also explains the relatively large difference in $\varepsilon_{235nm}(P_2)$ values from the two series (Table 3). In Series 1, one set of the kinetic data was recorded for almost 2 days, resulting much higher concentration of P_2, and thus, a reliable molar absorbance value. Mass spectrometric measurements of ampicillin samples hydrolyzed to a different extent revealed the identity of P_1 and P_2 products (Figure S3). P_1 is, as expected, the ampicilloic acid with an m/z value of the monoprotonated species of 368.1 being 18 units higher than that of the m/z value of ampicillin. This reveals a water uptake during the hydrolysis. The m/z value of the peak with increased relative intensity obtained for the sample expected to contain increased amount of P_2 was obtained to be 324.1. Accordingly, it is formed by the decarboxylation of P_1 at the carboxylic group established in the hydrolytic process. Such product was also identified previously in the studies of non-enzymatic ampicillin degradation and denoted as ampilloic acid (Mitchell et al., 2014; Sy et al., 2017; Raza Siddiqui et al., 2014; Robinson-Fuentes et al., 1997).

TABLE 3 Kinetic parameters and their standard deviations determined by the kinetic calculations for the hydrolysis of ampicillin including the processes catalyzed by TEM-1 β-lactamase and the further conversion of the first product (P_1) into the second product (P_2).

Parameter	Series 1	Series 2
k_1 (M^{-1} s^{-1})	$(4.34 \pm 0.12) \times 10^6$	$(4.81 \pm 0.30) \times 10^6$
k_2 (s^{-1})	$<1.4 \times 10^{-2}$	$<1.7 \times 10^{-2}$
k_3 (s^{-1})	$(2.24 \pm 0.03) \times 10^2$	$(3.44 \pm 0.01) \times 10^2$
k_4 (s^{-1})	$(7.50 \pm 0.18) \times 10^{-6}$	$(1.76 \pm 0.04) \times 10^{-5}$
$\varepsilon_{235\ nm}$ of Amp (M^{-1} cm^{-1})	1931 ± 2	1920 ± 1
$\varepsilon_{235\ nm}$ of P_1 (M^{-1} cm^{-1})	1064 ± 1.4	1081 ± 1
$\varepsilon_{235\ nm}$ of P_2 (M^{-1} cm^{-1})	709 ± 13	791 ± 5
K_M (μM)[a]	51.6 ± 1.4	71.6 ± 4.4
k_{cat}/K_M (μM^{-1} s^{-1})[a]	4.34 ± 0.12	4.81 ± 0.30

Note: The calculated ε_{235nm} values of the involved species are also provided. Series 1 are measurements conducted in 20 mM Tris–HCl (pH 7.5) buffer at 25°C, while the data in Series 2 were collected in 50 mM phosphate (pH 7.0) buffer at 30°C.

[a]These data were derived from the parameters obtained from the fitting procedure only for comparative purpose.

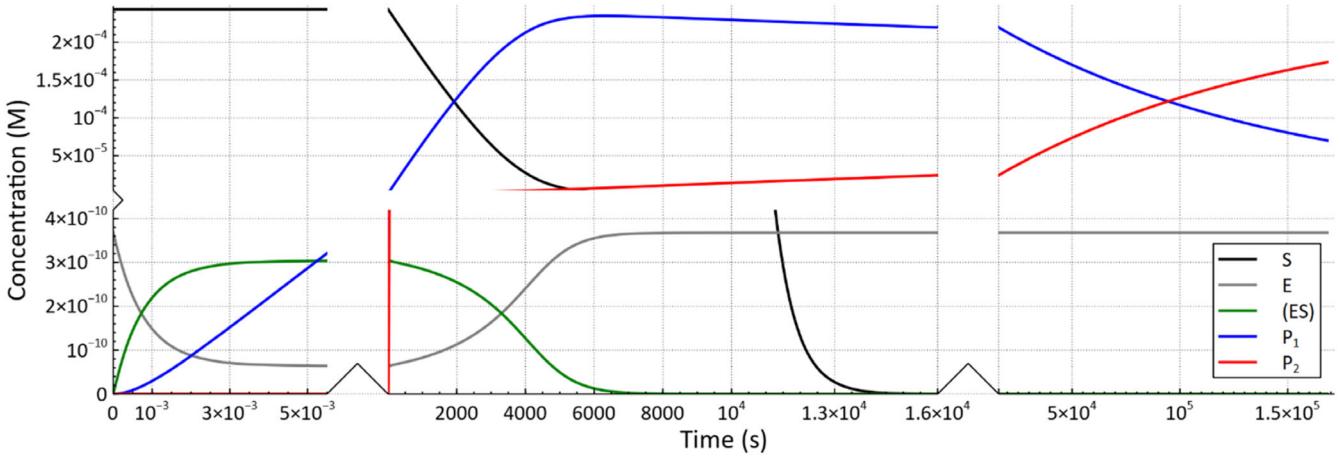

FIGURE 3 Distribution of species in the time course of the ampicillin hydrolysis, catalyzed by TEM-1 β-lactamase with $[S]_0 = 243$ μM and $[E]_0 = 0.37$ nM in 20 mM Tris–HCl (pH 7.5) buffer at 25°C followed for almost 2 days.

The relative amount of P_2 and therefore, its effect is certainly negligible at the very beginning of the reaction. Thus, it will not significantly influence the results obtained by the determination of initial rates, as long as the molar absorbance of the "product" can be determined properly. To show the advantage of the data evaluation, applied in this work, we have tried to determine the K_M values, using the usual Lineweaver–Burk plot, which would require a constant final absorbance (A_∞) value. This however, cannot be achieved in the TEM-1 β-lactamase/ampicillin system, due to slow but continuous absorbance decrease after the substrate has completely reacted. The formal application of this de facto standard procedure by choosing slightly variable A_∞ values revealed that the calculated K_M values are extremely sensitive to the choice of A_∞. The result is determined rather by the chosen value of A_∞ than by the experimental data as it is illustrated in Figure S4. In our example, 15% decrease in the A_∞ values resulted a 180% increase in the calculated K_M values. Additionally, the Lineweaver–Burk plot handles only one kinetic experiment at a single wavelength, while the kinetic evaluation procedure applied in this work handled all curves at all chosen wavelengths in a single run. Furthermore, this kind of kinetic description of the progress curves of the enzymatic reactions provides the precise molar absorbances at multiple wavelengths (Figure S2), as well as useful information about the alternative/consecutive transformation process influencing the values of the obtained parameters.

2.2 | The effect of metal ions on the catalytic activity of TEM-1 β-lactamase

Complexation of metal ions by TEM-1 β-lactamase may lead to change in the catalytic efficiency of the enzyme in promoting the hydrolysis of β-lactams. The ambiguity in the actual active enzyme concentration did not allow us to quantitatively evaluate the effect of the metal ions in successively performed catalytic experiments. Nevertheless, the experiments carried out concurrently with exactly the same diluted enzyme batches and substrate solutions under the same conditions, clearly demonstrated the effect of metal ions on the hydrolytic process. The results of the experiments carried out in the presence of increasing Hg(II) concentrations, as well as those containing different metal ions (Ni(II), Cd(II), and Hg(II)) at tenfold excess compared to the enzyme itself are shown in Figure 4.

The catalytic activity of TEM-1 β-lactamase was slightly reduced by the gradual increase of concentration of Hg(II) as shown in Figure 4a. This effect was observed in most of the experiments (>90%) carried out in the presence of Hg(II). These curves could be fitted allowing the change of the active enzyme concentration, yielding the same k_{cat} and K_M values as in the absence of Hg(II), but decreased V_{max} values in a correlation with the increased molar ratio of the metal ion and the enzyme. This suggests that the presence of Hg(II) does not affect the substrate binding, but influences the concentration of the catalytically effective enzyme possibly by blocking a fraction of the enzyme molecules. Based on these findings we hypothesize that Hg(II) may interact with the available sulfur donor atoms of Met residues thereby interfering with the catalytic process. A recent review draws the attention to the importance of methionine residues at various levels in proteins (Aledo, 2019). The network of methionines in TEM-1 β-lactamase including the distances between the sulfur donor atoms, as well as further amino acids with putative coordinating donor atoms found within a ~5 Å distance in the surroundings of each

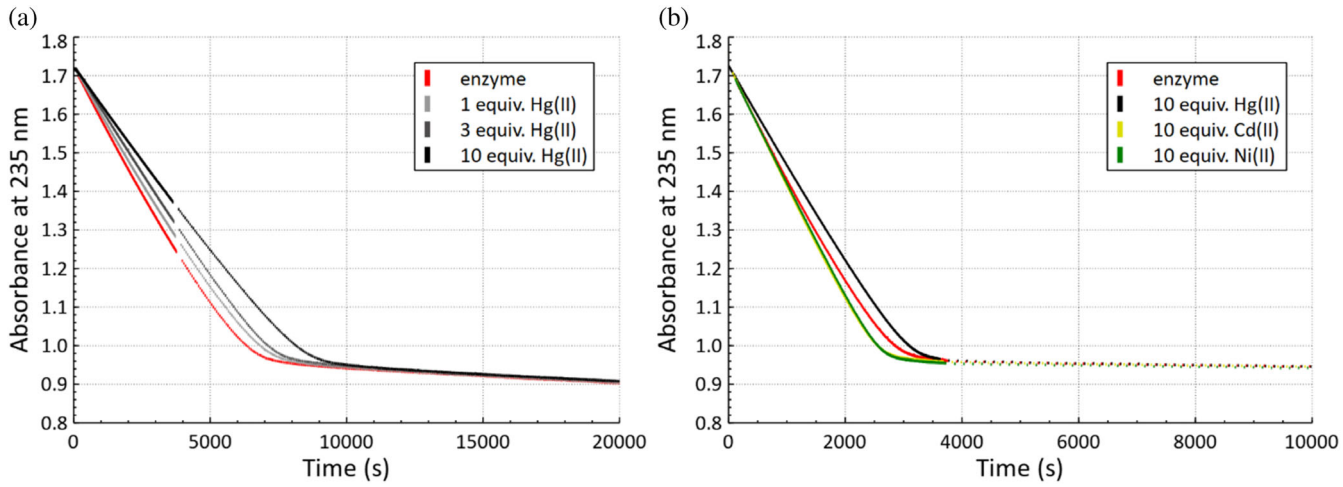

FIGURE 4 The effect of metal ions on the hydrolytic process of ampicillin catalyzed by TEM-1 β-lactamase in 50 mM phosphate buffer (pH 7.0) at 30°C. (a) The time dependence of the absorbances in parallel experiments hydrolyzing 900 μM ampicillin by ~0.8 nM enzyme in the presence of 1, 3 and 10 equivalents of Hg(II) referred to the enzyme concentration. (b) The kinetic curves recorded concurrently in the systems of 900 μM ampicillin and ~1.6 nM enzyme in the absence of metal ions, as well as with tenfold excess of Ni(II), Cd(II) and Hg(II) referred to the enzyme concentration.

methionine sulfur atom are collected in Figure 5. Amongst these residues, the two neighboring methionines (M68 and M69), located within a 6 Å sphere around the active center according to the published crystal structure (PDB id: 1zg4), may very likely offer the most stable binding site (Stec et al., 2005). Another favorable metal-binding site could be the donor atom-rich 129–132 (MSDN) segment including M129, which is within 8 Å surroundings of the active center. The importance of these sites in TEM-1 β-lactamase is supported by the sensitivity of the enzyme toward M68 and M69 mutations, while the 129-MSDN-132 sequence is in the mutation hotspot of the enzyme as previously demonstrated (Stiffler et al., 2015; Firnberg et al., 2014; Delaire et al., 1992).

In contrast to Hg(II), Ni(II) and Cd(II) seem to slightly promote the enzyme activity. This observation might not be surprising since ampicillin can also be hydrolyzed by metallo-β-lactamases (Bahr et al., 2021; Perez-Garcia et al., 2021) and metal ions are known to play significant role in enzyme catalyzed hydrolytic reactions (Huang et al., 2023). A metallo-β-lactamase with Cd(II) bound in its active center has also been found just a bit less active than the native Zn(II) enzyme itself supporting the ability of Cd(II) to promote the hydrolysis, while Hg(II) inhibited the function of this enzyme (Concha et al., 1997). Metal ions can even catalyze the hydrolysis of ampicillin, but mainly in strongly acidic or alkaline media. Such a reaction with Ni(II) in alkaline medium was applied for analytical purposes (Rašić-Mišić et al., 2013; Lin and Cen, 2022). On the other hand, we could not observe a significant change in the absorbance of ampicillin in the presence of Hg(II), Ni(II) or Cd(II) but absence of TEM-1 β-lactamase. Less than 0.01 absorbance unit decrease was detected within 3 h of incubation at identical concentrations and conditions to those applied in our kinetic assays (Figure S5). Nevertheless, the Lewis acid property of metal ions may help to hydrolyze the β-lactam ring by a different mechanistic pathway. The most probable scenario is the binding of the metal ion to the antibiotics with a concomitant activation of the substrate for the nucleophilic attack, which would also explain our observations (Gensmantel et al., 1980; Deshpande et al., 2004). Ni(II) and Cd(II), as borderline metal ions are supposed to bind ampicillin close to the β-lactam ring that would account for the behavior of these metal ions (Deshpande et al., 2004; El-Gamel, 2010). In contrast, Hg(II) may interact with the sulfur donor atoms (Deshpande et al., 2004), most probably resulting a much stronger interaction with the enzyme than with ampicillin.

2.3 | The influence of metal ions on bacterial growth

The presence of metal ions affects the bacterial resistance toward antibiotics in multiple ways. One of these might be the interaction with the antibiotic degrading enzymes, such as the TEM-1 β-lactamase. However, the behavior of bacteria in metal ion containing cultures is very complex. Synergism between heavy metal ions and β-lactam antibiotics in their action against bacteria were reported in the literature (Möhler et al., 2017; Garza-Cervantes

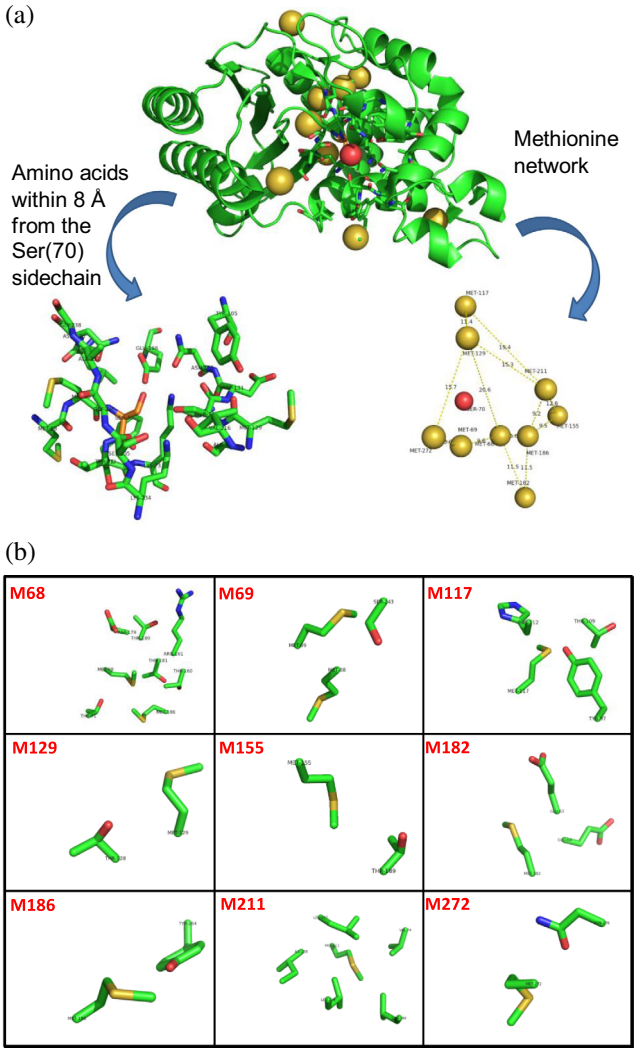

FIGURE 5 Structure of the TEM-1 β-lactamase (PDB id: 1zg4) highlighting the putative metal ion binding sites. (a) Coordinating amino acids with potential donor groups for metal ion coordination within 8 Å surroundings of the S70 sidechain and the network of methionines with distances between the sulfur donor atoms. (b) Amino acids containing further putative coordinating donor atoms in the 5 Å surroundings of each methionine sulfur.

et al., 2020), but there are also published experimental data demonstrating a parallel development of resistance against heavy metal ions and antibiotics (Chudobova et al., 2014; Wales and Davies, 2015; Wu et al., 2018; Vats et al., 2022). The degradation of β-lactam antibiotics in the presence of metal ions may also contribute to the decrease of their antimicrobial effect (Gensmantel et al., 1980; Deshpande et al., 2004). As an example, Cd(II) was reported to catalyze the degradation of ampicillin in methanol (García et al., 1998) or in Luria-Bertani bacterial growth medium (Beard et al., 1992). Nevertheless, the results are diverse and depend on many factors, such as the type of bacteria studied, the applied media and concentrations, etc. (Pavlić et al., 2022).

Because of the complexity of these systems we applied a well-controlled M9 minimal medium to monitor the effect of Hg(II), Ni(II), and Cd(II) on the viability of *E. coli* BL21 (DE3) bacterial cells. The cells were transformed with a modified pET-21a DNA vector providing ampicillin resistance. Therefore, ampicillin was non-toxic for bacteria at 270 μM concentration usually applied in our laboratory. It is worth to note that the sensitivity of the bacterial cultures toward the applied chemical agents was dependent on the initial number of the cells. The first series of experiments was carried out in bacterial cultures with low starting McFarland (1.0 McFarland unit stands for 3×10^8 viable cells/mL in the bacterial culture) values of ~1.0 (Figure S6). Various concentrations of Hg(II), Ni(II), or Cd(II), and/or ampicillin and isopropyl β-D-1-thiogalactopyranoside (IPTG) were added to these bacterial cultures and the changes of the McFarland values were recorded as the function of the incubation time. Cd(II) at 1.0 mM concentration proved to be slightly toxic for bacteria, while Ni(II) and Hg(II) did not allow the bacteria to proliferate at all at 1.0 and 0.5 mM concentrations, respectively (Figure S6a). The toxic effect of metal ions at these high concentrations was independent of the presence or absence of ampicillin. On decreasing the metal ion concentration to 10 μM, Cd(II) did not affect the bacterial growth. At the same time, neither Ni(II) nor Hg(II) allowed the bacteria to proliferate in these cultures. Surprisingly, a significant decrease of metal ion toxicity was observed when ampicillin was also present in the solutions (Figure S6b). Complex formation between metal ions and the antibiotics yielding adducts with a lower toxicity than that of the metal ions themselves could be an explanation of this observation. Although, there is an ambiguity in the literature about the stabilities of the complexes of these metal ions with ampicillin, generally a weak binding is suggested ($\log K_1 \sim 2$) (Fazakerley et al., 1976; Orabi, 2005; Zaworotko et al., 2006; Gupta, 2013). Nevertheless, metal complex formation may occur under the applied conditions, since ampicillin was applied at a high (27-fold) excess referred to metal ions in our systems. It has to be noted that the neutralization effect of ampicillin was more pronounced for Hg(II) than for Ni(II), which might be attributed to different coordination modes of the two metal ions in their ampicillin complexes as highlighted above. None of the applied metal ions were toxic for the bacteria at 1.0 μM concentrations with the exception of Hg(II), and this effect was also ceased by ampicillin (Figure S6b). On the other hand, parallel experiments (vide infra) using bacteria transformed with a DNA vector providing kanamycin resistance, demonstrated that the presence of this antibiotic could not protect the cells from the toxicity of the heavy metal ions.

The modified pET-21a DNA vector allowed for overexpression of TEM-1 β-lactamase upon inducing by IPTG.

The addition of IPTG to the above cultures, however, did not significantly influence the above observations on bacterial growth. The lysate of the collected bacterial pellets was analyzed by SDS PAGE (Figure S7). The overexpression of TEM-1 β-lactamase was attenuated in the presence of 10.0 μM Hg(II), and 10.0 μM Ni(II) in the presence of ampicillin, while it was completely inhibited at the same Hg(II) or Ni(II) concentrations in the absence ampicillin. Nevertheless, this might be attributed to the decreased viability of the bacteria, since the total protein content also decreased drastically. There was no change in the TEM-1 β-lactamase overexpression in samples containing Cd(II) at 1.0–10.0 μM concentrations.

In the second series of experiments the starting bacterial cultures exhibited ~2.3 McFarland values. Experiments without ampicillin were conducted to monitor the effect of metal ions. Under such conditions no effect of Ni(II), Cd(II) and Hg(II) ions at 1.0 μM concentration was observed on the bacterial growth (Figure 6). At increased concentrations (10.0 μM) only Hg(II) inhibited the bacterial growth significantly, but this effect could also be compensated by the addition of the antibiotics.

To further explore the interaction of the metal ions with antibiotics we have carried out the viability experiments with *E. coli* BL21 (DE3) bacteria transformed by the pET-M11-SUMO3-GFP DNA vector providing kanamycin resistance instead of ampicillin (Besir, 2017). Under such conditions Hg(II) was toxic, while Ni(II) was slightly toxic at 10.0 μM concentration and this effect was independent of the presence of kanamycin (Figure S8a).

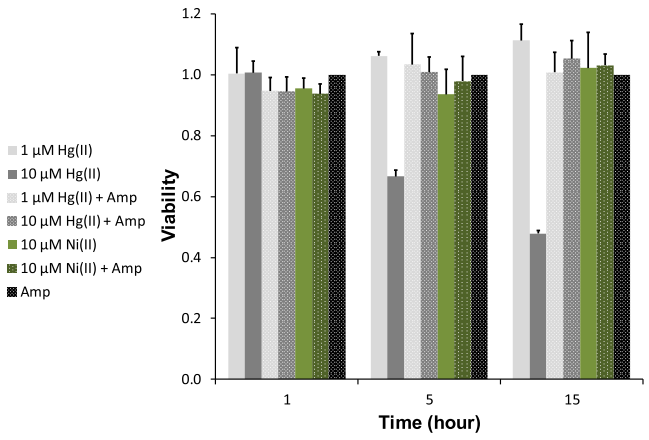

FIGURE 6 Viability of ampicillin resistant *E. coli* BL21 cells transformed with a modified pET-21a DNA vector in bacterial cultures grown in M9 minimal medium. The McFarland values of the culture grown in the presence of 270 μM ampicillin are compared with those obtained for the cultures containing metal ions at various concentrations. At each measurement point the viability was normalized to that of the cell culture containing only ampicillin as an added reagent.

Adding ampicillin to these bacterial cultures revealed that the antibiotics is not toxic at 10.0 μM, but already has a slight toxic effect at 100 μM concentration. These concentrations however, seem to be too small to affect the metal ion toxicity (Figure S8b). High excess of the antibiotics was needed to decrease the toxicity of the metal ions. This suggested that the stability of the complex formed between the metal ion and ampicillin is low in agreement with the literature data (Zaworotko et al., 2006).

2.4 | Interaction of metal ions with TEM-1 β-lactamase

The most significant effect on the catalytic activity of TEM-1 β-lactamase was observed with Hg(II). Therefore, we focused on this metal ion in the following experiments. ^{199m}Hg-PAC spectroscopy of γ-rays is a sensitive method for investigating the interaction of Hg(II) with the enzyme. PAC experiments were carried out in the presence of 0.9 eq. Hg(II) and 1.9 eq. Hg(II) with respect to TEM-1 β-lactamase, aiming to explore whether there is a well-defined high affinity binding site within the protein, and if so, to elucidate the coordination geometry Hg(II) occupies at such a site, as reflected in the nuclear quadrupole interaction (NQI). The NQI is mainly determined by two parameters, the quadrupole frequency, ν_Q, and the asymmetry parameter, η. In addition the parameter δ reflects the so-called static line broadening due to static (on the PAC time scale) variations in structure from one molecule to the next, λ reflects the effect of dynamics (local and global rotational diffusion), and the signal amplitude is denoted A (Hemmingsen et al., 2004). The data recorded for two reference samples ($Hg(Cys)_2$(s)) are also included in Table 4, because the two β-lactamase experiments were carried out on two different PAC instruments. The reference sample ensures that the frequency scales are properly aligned, and therefore that we can compare the measurements on TEM-1 β-lactamase samples. The reference gave the expected NQI for the experiments carried out on the digital PAC instrument (Jancsó et al., 2021), and the time-per-channel of the analogue PAC instrument was calibrated to give the same frequency.

The experimental data and Fourier transformed spectra are shown in Figure 7, and the fitted PAC parameters are presented in Table 4. Fitting with only one NQI, there are minor systematic deviations from the data, most notably in the range from 7 to 10 ns (fit not shown), where the fit undershoots the measured data. Therefore, two NQIs were included in the fitting procedure. One fraction of the signal, NQI_1, is an exponentially decaying

TABLE 4 Parameters fitted to ^{199m}Hg PAC data.

Sample	$c_{Hg(II)}$ (μM)	ν_Q (GHz)	η	δ ×100	λ (μs^{-1})	A ×100	χ_r^2
$Hg(Cys)_2$(s)	-	1.460 (5)	0.10 (8)	0.0 (7)	7 (8)	18.4 (9)	0.70
$Hg(Cys)_2$(s)	-	1.460[a]	0.10 (2)	0.0 (5)	3 (1)	14.4 (7)	0.70
TEM-1 β-lactamase	2.7	-	-	-	1.5 (6)[c]	8.9 (4)[b]	0.68
		1.35 (2)	0.21 (5)	9 (3)	0 (12)	7.4 (2)[b]	
TEM-1 β-lactamase	5.7	-	-	-	0.4 (2)[c]	4.0 (4)[b]	0.70
		1.39 (2)	0.18 (5)	12 (3)	0 (16)	10 (1)[b]	

Note: The experimental conditions were 3.0 μM TEM-1 β-lactamase, 10 mM HEPES (pH 7.4), 50% (w/w) sucrose, 1°C. $Hg(Cys)_2$(s) is a reference sample (Jancsó et al., 2021), and the data sets were recorded on a digital (first and third rows) and an analogue PAC instrument (second and fourth rows). The indicated errors (in parenthesis) are obtained from the statistical analysis of the data, and not from repetition of the experiments.

[a]Calibrated for the analogue instrument to be the same as for the digital instrument.

[b]The amplitudes are sensitive to the value of λ for the "fast" component (1.5(6) μs^{-1} and 0.4(2) μs^{-1}). The best fit is presented here but the amplitudes were not used for any quantitative conclusions.

[c]These rate parameters, λ, for the "fast" component, have a different physical meaning than the other values indicated in the same column, see Hemmingsen et al. (2004) for details.

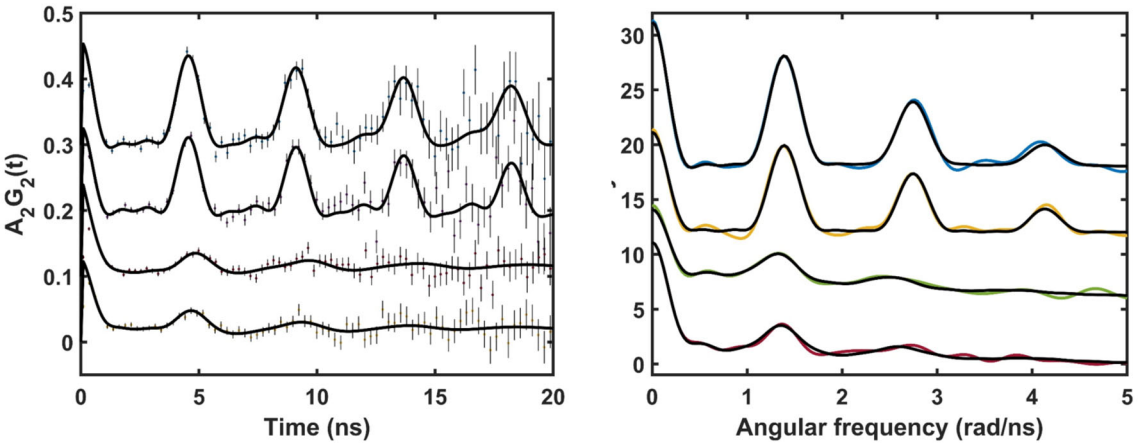

FIGURE 7 ^{199m}Hg PAC data. (Left) Experimental data and fit. Data points with error bars as 5-point average of raw data and fit as full line. (Right) Fourier transformed data (colored thin lines) and fit (black lines). From top to bottom: $Hg(Cys)_2$(s) reference recorded on the digital PAC instrument; $Hg(Cys)_2$(s) reference recorded on the analogue PAC instrument; 3 μM TEM-1 β-lactamase and 2.7 μM Hg(II); and 3 μM TEM-1 β-lactamase and 5.7 μM Hg(II); conditions for the latter two samples: 10 mM HEPES (pH 7.4), 50% (w/w) sucrose at 1°C.

component with no oscillatory time dependence, while the other, NQI_2, displays the damped oscillations that can be seen in Figure 7 (left part). It is reassuring that the total fitted amplitude, which must be constant for a given sample-detector geometry (and a given PAC probe), is approximately the same for the data recorded on each instrument for the reference samples and the TEM-1 β-lactamase. The exponentially decaying signal, NQI_1, must either reflect multiple binding sites and/or rapid dynamics, that is, it may reflect either free Hg(II) or Hg(II) non-specifically bound to TEM-1 β-lactamase. The parameter reflecting the rapid decay of the perturbation function, λ, is on the order of 1 μs^{-1}. Although this parameter appears to differ between the two experiments (1.5(6) and 0.4(2) μs^{-1}), it is possible to achieve a fit with the reversed values with only minor increase of the reduced chi-square. Accompanying this change, the amplitudes of the two signals change significantly. For example, fixing λ, to 0.4 μs^{-1} in the spectrum where it attains a value of 1.5 μs^{-1} when free in the fit, leads to a decrease in amplitude of NQI_1 to 0.04 and an increase in amplitude of NQI_2 to 0.12. In conclusion, the relative amplitudes of the two NQIs cannot be determined reliably. NQI_2 reflects a well-defined binding site (or several similar binding sites). The fact that oscillations are observed for this signal, demonstrates that dynamics at this binding site is in the so-called slow dynamics time regime ($\nu_Q \gg \lambda$), in agreement with the fitted value of $\lambda = 0$ μs^{-1}, with a statistical error bar of 12 and 16 μs^{-1} (see Table 4) in the two experiments. Using the extreme value of 16 μs^{-1}, and assuming that the dynamics is due only to rotational diffusion (and no local Hg(II) binding

site dynamics), we can derive a minimal molecular mass of the Hg(II) complex (see Fromsejer et al., 2023 and references therein). For this purpose we apply the Stokes–Einstein–Debye relation and a viscosity of 42 mPa s (50% (w/w) sucrose solution at 1°C), leading to a molecular mass >17 kDa, implying that Hg(II) is bound to a large molecule such as the protein or that it is precipitated. In terms of metal site structure, NQI_2 exhibits a relatively high frequency in the range in-between 2- and 3-coordinated Hg(II) complexes with thiolates as ligands (Iranzo et al., 2007). However, given that there are no free thiols, the ligands and coordination number are difficult to deduce unambiguously from the data. The relatively low asymmetry parameter, η, indicates that there is near axial symmetry, and one may speculate that the Hg(II) binding site could be a distorted linear two-coordinate or distorted trigonal planar structure with coordinating methionine(s) and/or histidine(s). Finally, given that both free (or non-specifically bound) Hg(II) and Hg(II) bound to a (or several similar) well defined binding site of the protein, are observed at the same time, the binding appears to occur to a binding site that does not have high affinity for Hg(II), but rather an apparent K_d on the order of μM.

Mass spectrometric experiments supported the above findings. Previously, we have found that TEM-1 β-lactamase could preferentially bind one Ni(II) and weakly a second Ni(II) most probably through the histidine sidechains exposed at the protein surface (Nafaee et al., 2023). In contrast to that, Hg(II) seems to interact weakly with TEM-1 β-lactamase. No specific Hg(II) adduct was detected by ESI MS. New peaks appeared at higher mass over charge (m/z) values in the systems containing TEM-1 β-lactamase and Hg(II) at increasing molar ratios. This suggested that the distribution of the complexes containing various number of Hg(II) at the multiple methionine binding sites is gradually shifted toward the oligometallated species upon increasing metal to protein ratio. Nevertheless, the free protein could be still detected even at fivefold metal ion excess. As it was described above (see Figure 5) there are methionines as sulfur-containing amino acids in the enzyme, few of them being close to the enzyme active center. The methionine thioether groups offer several binding sites for the soft metal ion like Hg(II). However, these sites are not fully occupied by Hg(II) as it was also indicated by the PAC results.

The secondary structure of TEM-1 β-lactamase and its changes upon metalation were studied by circular dichroism spectroscopy. The histidine-type metal binding sites of TEM-1 β-lactamase exposed at the protein surface did not significantly affect the secondary structure of the enzyme upon Ni(II) binding (Nafaee et al., 2023). The same result was also found for Cd(II), having most probably identical coordination mode to that of Ni(II). The methionine-type metal binding sites are inside the protein and are good candidates for binding of the soft metal ions, like Hg(II). The change of the structure of TEM-1 β-lactamase upon interaction with Hg(II) was monitored by CD spectroscopy. Hg(II) binding to TEM-1 β-lactamase resulted in slight gradual change in the CD spectra on increasing the excess of the metal ion (Figure 8).

The calculation of the secondary structure composition of the putative Hg(II)–TEM-1 β-lactamase adducts form the CD spectra demonstrated a gradual decrease of the α-helix content upon increase of the Hg(II) concentration. Nevertheless, these results do not reflect a remarkable secondary structure change even in the presence of an increased amount of Hg(II). Thus, the inhibitory effect of

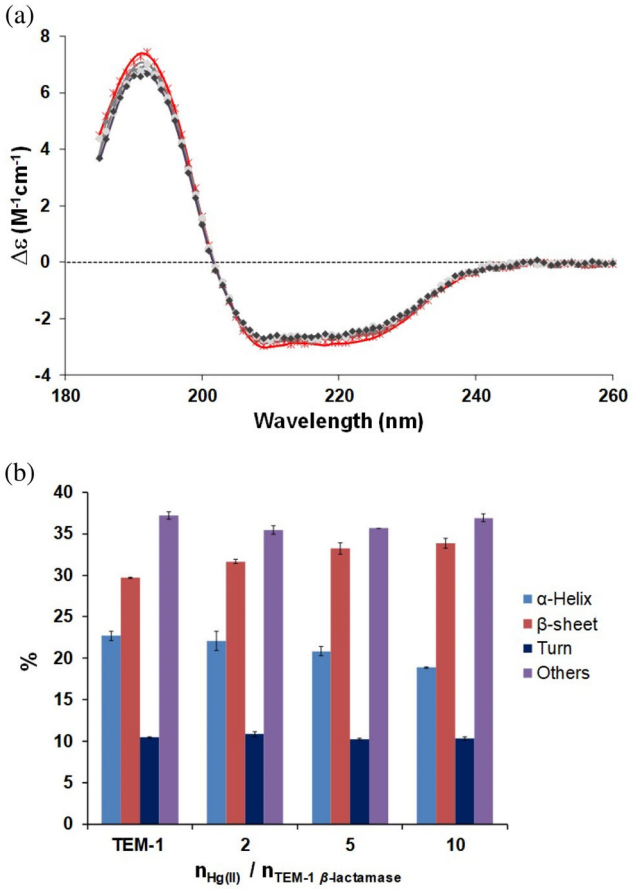

FIGURE 8 (a) Circular dichroism spectra of TEM-1 β-lactamase in 20 mM Tris–HCl (pH 7.5), in the presence of Hg(II) at different concentrations. (Hg(II):TEM-1 β-lactamase molar ratios were adjusted to 1:2, 1:5, and 1:10.) Symbols show the experimental points, while the lines represent their fit during the secondary structure calculations. (b) The fractions of the secondary structure elements of TEM-1 β-lactamase calculated from the circular dichroism spectra with the BeStSel program (Micsonai et al., 2015, 2018).

Hg(II) observed in the ampicillin hydrolysis experiments is rather attributed to its interaction with methionine amino acid residues close to the active center preventing them to actively participate in the catalytic process.

3 | CONCLUSIONS

The crystal structure of TEM-1 β-lactamase displays three putative histidine-pairs as metal binding sites on the protein surface and nine methionine sulfur donor atoms inside the protein. The CD spectra of the metallated TEM-1 β-lactamase did not significantly change upon interaction with metal ions. This indicates that the coordination of Ni(II), Cd(II) or Hg(II) to TEM-1 β-lactamase occurs without change of the secondary structure. Ni(II) has been shown previously by ESI-MS to bind to the enzyme, while we could not detect specific interaction of Hg(II) with the enzyme by this method. ^{199m}Hg perturbed angular correlation of γ-rays spectroscopy revealed that the metal ions are bound weakly to the protein presumably at interchangeable binding sites offered by methionine sidechains. We could not observe the influence of Cd(II) on the bacterial growth under the applied conditions. On the other hand, Ni(II) and Hg(II) were toxic for the bacteria at 10.0 and 1.0 μM, respectively in the absence of ampicillin. However, the addition of ampicillin to the bacterial cultures compensated for the toxic effect of the metal ions, presumably due to the formation complexes with no or less toxicity. The attenuation of metal ion toxicity by ampicillin was more successful for Hg(II) than for Ni(II), which can be related to different coordination modes of these metal ions in their ampicillin complexes. The kinetic description of the progress curves of ampicillin hydrolysis in the presence of TEM-1 β-lactamase revealed the necessity of a secondary hydrolysis product (P_2) identified to be penilloic acid. This kind of the data treatment also provided the opportunity to determine the molar absorbances of each species present in the system, as well as the precise concentration of the active enzyme at extremely low concentrations for which no other analytical methods are available. Metal ions exerted only a small effect on the catalytic activity of the enzyme in the test tube experiments. Hg(II) slightly inhibited, while the other two metal ions slightly promoted the catalytic reaction. This suggests that the TEM-1 β-lactamase/ampicillin catalytic system exhibits double selection of the applied metal ions through their interaction with both the enzyme and the substrate. Hg(II) is an antagonist for both the enzyme and the substrate through its interactions with the sulfur donor atoms. At the same time, Ni(II) and Cd(II) do not influence the structure/catalytic activity of the enzyme when they are bound to the surface histidines, while they activate ampicillin for hydrolysis by their coordination close to the beta lactam ring. To better understand the role of metal ions in this catalytic process, detailed mechanistic studies are planned in the future, which may reveal some of the individual reaction steps. In our hope these results will lead to the efficient design of future drugs/inhibitors or artificial enzymes.

4 | MATERIALS AND METHODS

4.1 | Reagents

All the reagents were used as purchased, without further purification. Reagents were obtained as follows: $NiCl_2$, $CdCl_2$ and $HgCl_2$, Na_2HPO_4, NaH_2PO_4, NH_4Cl, glucose, LB medium (Reanal, Budapest), NaCl (Szkarabeusz Laboratóriumi, Vegyipari és Kereskedelmi kft), KCl, tris(hydroxymethyl)aminomethane (Molar Chemicals), imidazole, ammonium bicarbonate (Sigma-Aldrich), tricine (VWR Life Science), isopropyl β-D-1-thiogalactopyranoside (IPTG), dioxane free (Thermo Scientific), pET-21a (Novagen). Seakem LE agarose was Lonza, Rockland, ME product, acrylamide/bis-acrylamide (29/1) as a 30% (w/v) solution, ampicillin and kanamycin were SERVA Electrophoresis GmbH, Heidelberg products. *E. coli* DH10B F^- end A1 recA1 galU galK deoR nupG rpsL ΔlacX74 *Φ*80lacZΔM15 araD139 Δ(ara,leu)7697 mcrA Δ (mrr-hsdRMS-mcrBC) λ^- was used for cloning (Grant et al., 1990) while *E. coli* BL21 (DE3) F^- ompT gal [dcm] [lon] $hsdS_B$ for protein expression (Studier et al., 1990).

4.2 | Protein purification

TEM-1 β-lactamase was purified in two steps of immobilized metal ion affinity chromatography (IMAC) and in a subsequent step of anion exchange chromatography (Figure S9) according to the previously described protocol (Nafaee et al., 2023). For IMAC, a Ni(II)-loaded Sepharose 6 Fast Flow resin in XK 16/20 column, and for anion exchange a HiPrep Q Sepharose FF anion-exchanger were applied with an ÄKTA FPLC explorer system (GE Healthcare/Bio-Science AB products). The sodium dodecyl sulfate polyacrylamide gel electrophoresis (SDS-PAGE) examination of the final product approved the purity of the target protein (Figure S9). The concentration of TEM-1 β-lactamase (in 20 mM Tris–HCl (pH 7.5)) was determined spectroscopically based on $\varepsilon_{280nm} = 28{,}085\ M^{-1}\ cm^{-1}$ (obtained via Expasy online tool [https://web.expasy.org/protparam/]).

4.3 | Determination of activity, and kinetic parameters

Kinetic parameters of purified TEM-1 β-lactamase were determined by the analysis of UV absorption spectrometric data collected during the hydrolysis of the ampicillin samples. A series of ampicillin substrate solutions with concentrations of 230 or 930 μM were prepared in 1–1 mL 20 mM Tris–HCl (pH 7.5) for Series 1 or in 1–1 mL 50 mM phosphate buffer (pH 7.0) for Series 2 experiments and then mixed with the purified enzyme (yielding 0.24–2.4 nM enzyme concentrations). The reactions were followed using a Cary 3500 UV–Vis double beam multi-cell spectrophotometer (Agilent Technologies) at 25°C (Series 1) or 30°C (Series 2) controlled temperature in the 210–235 nm wavelength interval in a narrow quartz cuvette (Hellma) with 1.0 cm path length.

The kinetic calculations were carried out by the program ChemMech (Peintler, 1989–2022), which has been developing specifically to fit more experimental curves simultaneously in a single run. This way, exactly the same value of every parameter was used during the simulation of the calculated curves. It is not true if the curves would be fitted separately. First, the concentration versus time curves were calculated with a specific set of rate constant values and initial concentrations as a particular solution of the differential equation system. It is the precise mathematical model of the mechanism given in Equation (1). There was not any simplification or modification of this equation system during the calculations. Empirical equations without chemical consideration were not used at all.

$$\begin{aligned}
\frac{d[\mathrm{S}]}{dt} &= -k_1\cdot[\mathrm{S}]\cdot[\mathrm{E}]+k_2\cdot[(\mathrm{ES})]\\
\frac{d[\mathrm{E}]}{dt} &= -k_1\cdot[\mathrm{S}]\cdot[\mathrm{E}]+(k_2+k_3)\cdot[(\mathrm{ES})]\\
\frac{d[(\mathrm{ES})]}{dt} &= +k_1\cdot[\mathrm{S}]\cdot[\mathrm{E}]-(k_2+k_3)\cdot[(\mathrm{ES})]\\
\frac{d[\mathrm{P_1}]}{dt} &= +k_3\cdot[(\mathrm{ES})]-k_4\cdot[\mathrm{P_1}]\\
\frac{d[\mathrm{P_2}]}{dt} &= +k_4\cdot[\mathrm{P_1}]
\end{aligned}$$

From the calculated $c(t)$ curves. The absorbance versus time curves (analogous to the kinetic experiments) can be computed by the use of Beer–Lambert law with an appropriate set of molar absorbance values. After this the fitting meant to an automatic change in the rate constants and molar absorbance values and recalculation of the $A(t)$ curves until reaching the minimal difference between the measured and calculated curves.

During the calculations, the number of time points was reduced to 120 for each curve to weight them equally. They were distributed along the arc of the curves as proportionally as possible so the information content of the whole monitored time range was included in the calculations. The final set of the fitted parameters are given in Table 3. This fitting procedure was carried out in several ways (e.g., changing the fitted and fixed parameters), and finally it was proven that adding one more step (namely the last step in Equation (1)) to the hypothesized minimal model is sufficient to describe the measured curves within the experimental uncertainty. Of course, more steps might exist but there is not enough experimental information in our data set to determine further processes.

4.4 | Bacterial viability assay

Viability of *E. coli* BL21(DE3) cells in the presence of metal ions (Hg(II), Cd(II), or Ni(II)) was assessed in M9 minimal medium (Miller, 1972). McFarland values. Bacteria were transformed with a modified pET-21a vector (Nafaee et al., 2023) providing ampicillin resistance in experiments 1–7 and while with the pET-M11-SUMO3-GFP DNA vector providing kanamycin resistance (Besir, 2017) in experiments 8–11 and grown in 50 mL ampicillin containing lysogeny broth (LB) media at 37°C (Table 5). The bacterial cultures displaying ∼2.6 McFarland value, were centrifuged at 4000 × *g* for 15 min at 4°C. The pellets were washed twice with cold M9 minimal medium and then resuspended in M9 minimal medium. These bacterial cultures were distributed into 5 mL aliquots and incubated with shaking at 37°C until a McFarland value of ∼1.0 (experiments 1–5) or ∼2.3 (experiments 6–11) was reached. The chemical solutions (ampicillin, kanamycin, IPTG, and metal ions) were added at various concentrations (Table 5), and then the samples were incubated at 24°C for up to 17 h.

4.5 | Investigation of the TEM-1 β-lactamase overexpression in the presence of metal ions

Overexpression of TEM-1 β-lactamase in bacteria grown in metal ion containing M9 media was identified by 12–15% (w/v) SDS-PAGE. A mixture of seven unstained proteins (116, 66.2, 45, 35, 25, 18.4, and 14.4 kDa) served as a molecular marker (Thermo Scientific). The electrophoresis experiments were carried out at room temperature at 70 V for 30 min, then at 120 V for 150–180 min, using 0.1 M Tris–HCl, 0.1 M tricine, 0.1% (w/v) SDS (pH 8.3) as

TABLE 5 Conditions of bacterial viability experiments.

Experiments no.	1	2–4	5	6, 7	8, 9	10, 11
Starting McFarland value	~1.0	~1.0	~1.0	~2.3	~2.3	~2.3
Ampicillin (μM)	0 or 270	0 or 270	0 or 270	0 or 270	–	10 or 100
Kanamycin (μM)	–	–	–	–	0 or 83	0 or 83
IPTG (mM)	–	–	0 or 1.0	0 or 1.0	–	–
Ni(II) (μM)	1000	1.0 or 10.0	1.0 or 10.0	1.0 or 10.0	1.0 or 10.0	–
Cd(II) (μM)	1000	1.0 or 10.0	1.0 or 10.0	1.0 or 10.0	1.0 or 10.0	–
Hg(II) (μM)	500	1.0 or 10.0	1.0 or 10.0	1.0 or 10.0	1.0 or 10.0	5.0–100.0

the cathode buffer and 0.2 M Tris–HCl (pH 8.9) as the anode buffer.

4.6 | Mass spectrometric analysis

Intact protein analysis was achieved by high resolution mass spectrometry. Intact protein mass measurement was carried out on a Nanomate TriVersa (Advion) chip-based nanoelectrospray ion source coupled to a LTQ-Orbitrap Elite mass spectrometer (ThermoFisher). The protein concentration was 2.0 μM in each individual sample containing 0, 2, 5, and 10 equivalents of $HgCl_2$. The samples were buffered at pH 7.8 with a solution containing 50 mM ammonium bicarbonate/NH_3(aq).

4.7 | Circular dichroism spectroscopic measurements

CD spectra were recorded at room temperature by a Jasco J-1500 CD spectrometer. The parameters were adjusted as described in the following. Wavelength range: 300–180 nm; path length: 0.2 mm (Hellma quartz cuvette); DIT: 2 s; bandwidth: 1.0 nm; scanning speed: 50 nm/min (continuous scanning mode). The concentration of TEM-1 β-lactamase was 8.6 μM in 20 mM Tris–HCl (pH 7.5). TEM-1 β-lactamase was titrated with Cd(II) and Hg(II) to adjust protein:M(II) molar ratios to 1:2, 1:5 and 1:10.

4.8 | PAC measurements

^{199m}Hg PAC measurements were performed at the ISOLDE laboratories at CERN (Catherall et al., 2017). Radioactive mercury was produced and collected in ~150 μL of frozen milliQ water, as described previously (Jancsó et al., 2021).

TABLE 6 Sample preparation for ^{199m}Hg PAC measurements.

Stock solutions	Sample 1	Sample 2
Hot Hg(II)	140 μL	
Cold Hg(II) (100 μM $HgCl_2$ solution)	13.5 μL	28.5 μL
500 mM HEPES buffer (pH 7.4)	10 μL	
~23.1 μM TEM-1 β-lactamase in 20 mM Tris–HCl (pH 7.5)	65 μL	
0.1 M $HClO_4$	23 μL	
H_2O (and acid/base for pH adjustment)	56 μL	41 μL
V_{total}	307.5 μL	
Sucrose	0.3075 g	
V_{final}	500 μL	
Density of 50% (w/w) sucrose solution	1.23 g/mL	

4.8.1 | Preparation of the samples

The following solutions were used for sample preparation (Table 6): 0.3 mL of 23.1 μM TEM-1 β-lactamase protein stock solution in 20 mM Tris–HCl (pH 7.5); 100 μM $HgCl_2$ stock solution; 500 mM HEPES buffer solution (pH 7.4) and stock solutions for pH adjustment (1.0 M NaOH, 1.0 M $HClO_4$, 0.1 M NaOH, 0.1 M $HClO_4$). Sample 1 contained 3.0 μM TEM-1 β-lactamase and 2.7 μM Hg(II) in 10 mM HEPES (pH 7.4), 50% (w/w) sucrose. Sample 2 contained 3.0 μM TEM-1 β-lactamase and 5.7 μM Hg(II) in 10 mM HEPES (pH 7.4), 50% (w/w) sucrose.

4.8.2 | PAC instruments and data analysis

Two PAC setups were used, the digital DIGIPAC (Jäger et al., 2011) equipped with six 1.5 in. × 1.5 in. $LaBr_3$(Ce) detectors and the analogue PERM (Butz et al., 1989) with six 1 in. × 1 in. $CeBr_3$ detectors. Time

resolutions of 0.6 and 0.5 ns, respectively were obtained by averaging the values obtained during determination of t_0 channels for the 30 individual spectra of detector pairs in the 6-detector setups. Time-per-channel calibrations of 0.04883 and 0.05068 ns were used for the digital and analogue PAC setups, respectively (calibrated so as to give the same recorded frequency for the $Hg(Cys)_2$(s) sample for the two instruments).

Data analysis was carried out with the Winfit program (provided by prof. T. Butz) using 600 data points (excluding the first 10 points due to t_0 determination uncertainties near time zero). A Lorentzian line shape was used to account for line broadening, given by the parameter δ, due to a static distribution of EFGs. Fourier transformation of the data and fits were carried out using 600 points after mirroring 300 data points and a Kaiser–Bessel function with the window parameter equal to 4.

For nuclear spin $I = 5/2$ (which is the case for the intermediate nuclear state for which the NQI is measured in ^{199m}Hg PAC) and randomly oriented, static, identical Hg(II) sites, the so-called perturbation function (Frauenfelder and Steffen, 1965; Hemmingsen et al., 2004) is given by:

$$A_{22}^{\text{eff}} G_{22}(t) = A_{22}^{\text{eff}} (a_0 + a_1 \cos(\omega_1 t) + a_2 \cos(\omega_2 t) + a_3 \cos(\omega_3 t))$$

where $A_{22}{}^{\text{eff}}$ is the effective anisotropy, and a_i and ω_i depend on the NQI (Butz, 1989, 1992).

The experimental equivalent of $A_{22}{}^{\text{eff}} G_{22}(t)$, $R(t)$, is constructed as (Hemmingsen et al., 2004):

$$R(t) = 2\frac{W(180^\circ, t) - W(90^\circ, t)}{W(180^\circ, t) + 2W(90^\circ, t)}$$

where $W(180^\circ,t)$ and $W(90^\circ,t)$ are the geometrical mean of coincidence spectra recorded with 180° and 90° between detectors, after subtraction of random coincidences and adjustment to the same time = 0 for all 30 coincidence time traces. The data presented in Figure 7 have been base-line shifted to 0. This has no effect on the fitted parameters.

AUTHOR CONTRIBUTIONS

Zeyad H. Nafaee: Protein expression and purification (lead); kinetic experiments (lead); CD measurements and evaluation (equal); writing – original draft (lead). **Viktória Egyed:** CD measurements and evaluation (equal); kinetic measurements (supporting); visualization (supporting). **Attila Jancsó:** PAC experiments (lead), kinetic evaluation (supporting); writing – review and editing (equal). **Annamária Tóth:** PAC experiments (equal). **Adeleh Mokhles Gerami:** PAC experiments (equal). **Thanh Thien Dang:** PAC experiments (equal). **Juliana Schell:** PAC experiments (equal). **Lars Hemmingsen:** Data curation (equal), PAC evaluation (lead), writing PAC section (lead); funding acquisition (equal). **Éva Hunyadi-Gulyás:** Data curation (equal); MS evaluation (lead). **Gábor Peintler:** Data curation (equal), kinetic evaluation (lead); writing – review and editing (equal). **Béla Gyurcsik:** Conceptualization (lead); supervision (lead); data curation (lead); writing – review and editing (equal); funding acquisition (equal).

ACKNOWLEDGMENTS

This research was supported by the Hungarian National Research, Development and Innovation Office (GINOP-2.3.2-15-2016-00038, GINOP-2.3.2-15-2016-00001, GINOP-2.3.2-15-2016-00020, and 2019-2.1111-TÉT-2019-00089). We acknowledge the financial support received from the Federal Ministry of Education and Research (BMBF) through grants 05K16PGA and 05K22PGA. We also thank the European Union's Horizon Europe Framework research and innovation programme under grant agreement no. 101057511 (EURO-LABS) and the European Union's Horizon 2020 Framework research and innovation program under grant agreement no. 654002 (ENSAR2). Funding project CERN-FIS-PAR-0005-2017 FCT-Portugal is acknowledged in support of the analogue PAC setup and of the new implantation chamber for icy samples. We thank CERN and the ISOLDE technical team for beam time, EURONS and NICE for financial support.

CONFLICT OF INTEREST STATEMENT

The authors declare no conflicts of interest.

DATA AVAILABILITY STATEMENT

The main data supporting findings of this study are available within the article and Supplementary Material. Additional data are available from the corresponding author on request.

ORCID

Béla Gyurcsik https://orcid.org/0000-0003-1894-7414

REFERENCES

Aledo JC. Methionine in proteins: the Cinderella of the proteinogenic amino acids. Protein Sci. 2019;28:1785–96.

Ambler RP, Coulson AF, Frère JM, Ghuysen JM, Joris B, Forsman M, et al. A standard numbering scheme for the class A β-lactamases. Biochem J. 1991;276:269–70.

Bahr G, González LJ, Vila AJ. Metallo-β-lactamases in the age of multidrug resistance: from structure and mechanism to evolution, dissemination, and inhibitor design. Chem Rev. 2021;121:7957–8094.

Besir H. A generic protocol for purifying disulfide-bonded domains and random protein fragments using fusion proteins with

SUMO3 and cleavage by SenP2 protease. Methods Mol Biol. 2017;1586:141–54.

Birgersson B, Drakenberg T, Neville GA. Mercury(II) complexes of methionine. Acta Chem Scand. 1973;27:3953–60.

Beard SJ, Ciccognani DT, Hughes MN, Poole RK. Metal ion-catalysed hydrolysis of ampicillin in microbiological growth media. FEMS Microbiol Lett. 1992;96:207–12.

Birgy A, Magnan M, Hobson CA, Figliuzzi M, Panigoni K, Codde C, et al. Local and global protein interactions contribute to residue entrenchment in beta-lactamase TEM-1. Antibiotics. 2022;11:652.

Bratulic S, Gerber F, Wagner A. Mistranslation drives the evolution of robustness in TEM-1 β-lactamase. Proc Natl Acad Sci U S A. 2015;112:12758–63.

Brown NG, Shanker S, Prasad BVV, Palzkill T. Structural and biochemical evidence that a TEM-1 β-lactamase N170G active site mutant acts via substrate-assisted catalysis. J Biol Chem. 2009;284:33703–12.

Brown PR, Edwards JO. Reaction of disulfides with mercuric ions. Biochemistry. 1969;8:1200–2.

Bush K, Jacoby GA, Medeiros AA. A functional classification scheme for beta-lactamases and its correlation with molecular-structure. Antimicrob Agents Chemother. 1995;39:1211–33.

Bush K, Jacoby GA. Updated functional classification of β-lactamases. Antimicrob Agents Chemother. 2010;54:969–76.

Butz T, Saibene S, Fraenzke T, Weber M. A "TDPAC-camera". Nucl Instr Meth Phys Res. 1989;A284:417–21.

Butz T. Analytic perturbation functions for static interactions in perturbed angular correlations of γ-rays. Hyperfine Interact. 1989;52:189–228.

Butz T. Analytic perturbation functions for static interactions in perturbed angular correlations of γ-rays. Hyperfine Interact. 1992;73:387–8.

Cantu C, Huang W, Palzkill T. Cephalosporin substrate specificity determinants of TEM-1 β-lactamase. J Biol Chem. 1997;272:29144–50.

Carty AJ, Taylor NJ. Binding of inorganic mercury at biological sites: crystal structures of Hg^{2+} complexes with sulphur amino-acids. J Chem Soc Chem Commun. 1976;(6):214–6.

Catherall R, Andreazza W, Breitenfeldt M, Dorsival A, Focker GJ, Gharsa TP, et al. The ISOLDE facility. J Phys G. 2017;44:94002.

Chudobova D, Dostalova S, Blazkova I, Michalek P, Ruttkay-Nedecky B, Sklenar M, et al. Effect of ampicillin, streptomycin, penicillin and tetracycline on metal resistant and non-resistant Staphylococcus aureus. Int J Environ Res Public Health. 2014;11:3233–55.

Citri N, Samuni A, Zyk N. Acquisition of substrate-specific parameters during the catalytic reaction of penicillinase. Proc Natl Acad Sci U S A. 1976;73:1048–52.

Concha NO, Rasmussen BA, Bush K, Herzberg O. Crystal structures of the cadmium- and mercury-substituted metallo-beta-lactamase from Bacteroides fragilis. Protein Sci. 1997;6:2671–6.

Cumming AJ, Khananisho D, Harris R, Bayer CN, Nørholm MHH, Jamshidi S, et al. Antibiotic-efficient genetic cassette for the TEM-1 β-lactamase that improves plasmid performance. ACS Synth Biol. 2022;11:241–53.

Damblon C, Raquet X, Lian LY, Lamotte-Brasseur J, Fonze E, Charlier P, et al. The catalytic mechanism of beta lactamases: NMR titration of an active-site lysine residue of the TEM-1 enzyme. Proc Natl Acad Sci U S A. 1996;93:1747–52.

Delaire M, Labia R, Samama JP, Masson JM. Site-directed mutagenesis at the active site of Escherichia coli TEM-1 beta-lactamase. Suicide inhibitor-resistant mutants reveal the role of arginine 244 and methionine 69 in catalysis. J Biol Chem. 1992;267:20600–6.

Dellus-Gur E, Elias M, Caselli E, Prati F, Salverda MLM, Arjan J, et al. Negative epistasis and evolvability in TEM-1 β-lactamase – the thin line between an enzyme's conformational freedom and disorder. J Mol Biol. 2015;427:2396–409.

Deshpande AD, Baheti KG, Chatterjee NR. Degradation of β-lactam antibiotics. Curr Sci. 2004;87:1684–95.

Egorov A, Rubtsova M, Grigorenko V, Uporov I, Veselovsky A. The role of the Ω-loop in regulation of the catalytic activity of TEM-type β-lactamases. Biomolecules. 2019;9:854.

El-Gamel NEA. Metal chelates of ampicillin versus amoxicillin: synthesis, structural investigation, and biological studies. J Coord Chem. 2010;63:534–43.

Fazakerley GV, Jackson GE, Linder PW. Equilibrium studies of benzylpenicillinate-thiaprolinate-hippurate- and benzylpenicilloate-proton and transition metal(II) ion systems. J Inorg Nucl Chem. 1976;38:1397–400.

Firnberg E, Labonte JW, Gray JJ, Ostermeier M. A comprehensive, high-resolution map of a gene's fitness landscape. Mol Biol Evol. 2014;31:1581–92.

Fragoso A, Lamosa P, Delgado R, Iranzo O. Harnessing the flexibility of peptidic scaffolds to control their copper(II)-coordination properties: a potentiometric and spectroscopic study. Chem A Eur J. 2013;19:2076–88.

Frauenfelder H, Steffen RM. Alpha-, beta and gamma-ray spectroscopy. Amsterdam: North Holland; 1965. p. 997.

Fromsejer R, Jensen ML, Zacate MO, Karner VL, Pecoraro VL, Hemmingsen L. Molecular rotational correlation times and nanoviscosity determined by ^{111m}Cd perturbed angular correlation (PAC) of γ-rays spectroscopy. Chem A Eur J. 2023;29:e202203084.

Furey IM, Mehta SC, Sankaran B, Hu L, Prasad BVV, Palzkill T. Local interactions with the Glu166 base and the conformation of an active site loop play key roles in carbapenem hydrolysis by the KPC-2 β-lactamase. J Biol Chem. 2021;296:100799.

Galleni M, Frère J-M. Kinetics of β-lactamases and penicillin-binding proteins. In: Bonomo RA, Tolmasky M, editors. Enzyme-mediated resistance to antibiotics: mechanisms, dissemination, and prospects for inhibition. Washington, DC: ASM Press; 2007.

García AM, Navarro PG, Martínez de las Parras PJ. Degradation of ampicillin in the presence of cadmium(II) ions. Talanta. 1998;46:101–9.

Garza-Cervantes JA, Meza-Bustillos JF, Resendiz-Hernández H, Suárez-Cantú IA, Ortega-Rivera OA, Salinas E, et al. Re-sensitizing ampicillin and kanamycin-resistant *E. coli* and *S. aureus* using synergistic metal micronutrients-antibiotic combinations. Front Bioeng Biotechnol. 2020;8:612.

Gensmantel NG, Proctor P, Page MI. Metal-ion catalysed hydrolysis of some β-lactam antibiotics. J Chem Soc Perkin Trans. 1980;2:1725–32.

Grant SG, Jessee J, Bloom FR, Hanahan D. Differential plasmid rescue from transgenic mouse DNAs into Escherichia coli

methylation-restriction mutants. Proc Natl Acad Sci U S A. 1990;87:4645–9.

Gupta A. Stability constant and thermodynamic parameters determination of a semi-synthetic penicillin derivative with various bivalent metal ions (Co^{2+}, Ni^{2+}, Cu^{2+}, Zn^{2+}, Cd^{2+}, Sn^{2+}, Hg^{2+} and Pb^{2+}): a potentiometric study. Int Res J Pure Appl Chem. 2013;3:441–8.

Hemmingsen L, Sas KN, Danielsen E. Biological applications of perturbed angular correlations of γ-ray spectroscopy. Chem Rev. 2004;104:4027–61.

Huang J, Liu X, Sun Y, Li Z, Lin MH, Hamilton K, et al. An examination of the metal ion content in the active sites of human endonucleases CPSF73 and INTS11. J Biol Chem. 2023;299: 103047.

Huang W, Palzkill T. A natural polymorphism in β-lactamase is a global suppressor. Proc Natl Acad Sci U S A. 1997;94:8801–6.

Huang W, Petrosino J, Hirsch M, Shenkin PS, Palzkill T. Amino acid sequence determinants of β-lactamase structure and activity. J Mol Biol. 1996;258:688–703.

Iranzo O, Thulstrup PW, Ryu S, Hemmingsen L, Pecoraro VL. The application of ^{199}Hg NMR and ^{199m}Hg perturbed angular correlation (PAC) spectroscopy to define the biological chemistry of Hg^{II}: a case study with designed two- and three-stranded coiled coils. Chem A Eur J. 2007;13:9178–90.

Jacquier H, Birgy A, Le Nagarda H, Mechulam Y, Schmitt E, Glodt J, et al. Capturing the mutational landscape of the beta-lactamase TEM-1. Proc Natl Acad Sci U S A. 2013;110: 13067–72.

Jäger M, Iwig K, Butz T. A compact digital time differential perturbed angular correlation-spectrometer using field programmable gate arrays and various timestamp algorithms. Rev Sci Instr. 2011;82:065105.

Jancsó A, Correia JG, Balogh RK, Schell J, Jensen ML, Szunyogh D, et al. A reference compound for ^{199m}Hg perturbed angular correlation of γ-rays spectroscopy. Nucl Inst Meth Phys Res. 2021; 1002:165154.

Judge A, Hu L, Sankaran B, Van Riper J, Venkataram Prasad BV, Palzkill T. Mapping the determinants of catalysis and substrate specificity of the antibiotic resistance enzyme CTX-M β-lactamase. Commun Biol. 2023;6(1):35.

Jullien A-S, Gateau C, Lebrun C, Delangle P. Pseudo-peptides based on methyl cysteine or methionine inspired from Mets motifs found in the copper transporter Ctr1. Inorg Chem. 2015;54: 2339–44.

Kather I, Jakob RP, Dobbek H, Schmid FX. Increased folding stability of TEM-1 β-lactamase by in vitro selection. J Mol Biol. 2008; 383:238–51.

Latha MP, Rao VM, Rao TS, Rao GN. Chemical speciation of Pb(II), Cd(II), Hg(II), Co(II), Ni(II), Cu(II) and Zn(II) binary complexes of L-methionine in 1,2-propanediol–water mixtures. Bull Chem Soc Ethiop. 2007;21:363–72.

Lawung R, Prachayasittikul V, Low LB. Purification and characterization of a β-lactamase from Haemophilus ducreyi in *Escherichia coli*. Protein Expr Purif. 2001;23:151–8.

Lenz GR, Martell AE. Metal chelates of some sulfur-containing amino acids. Biochemistry. 1964;3:745–50.

Lin Y, Cen S. Content determination of ampicillin by Ni(II)-mediated UV-vis spectrophotometry. RSC Adv. 2022;12: 9786–92.

Lund BA, Christopeit T, Guttormsen Y, Bayer A, Leiros HK. Screening and design of inhibitor scaffolds for the antibiotic resistance oxacillinase-48 (OXA-48) through surface plasmon resonance screening. J Med Chem. 2016;59:5542–54.

Madzgalla S, Duering H, Hey JC, Neubauer S, Feller KH, Ehricht R, et al. Assessment of phenotype relevant amino acid residues in TEM-β-lactamases by mathematical modelling and experimental approval. Microorganisms. 2021;9:1726.

Marciano DC, Brown NG, Palzkill T. Analysis of the plasticity of location of the Arg244 positive charge within the active site of the TEM-1 β-lactamase. Protein Sci. 2009;18:2080–9.

Massova I, Mobashery S. Kinship and diversification of bacterial penicillin-binding proteins and beta-lactamases. Antimicrob Agents Chemother. 1998;42:1–17.

Matagne A, Frère J-M. Contribution of mutant analysis to the understanding of enzyme catalysis: the case of class A β-lactamases. Biochim Biophys Acta. 1995;1246:109–27.

Matagne A, Lamotte-Brasseur J, Frère J-M. Catalytic properties of class A β-lactamases: efficiency and diversity. Biochem J. 1998; 330:581–98.

Mehta SC, Furey IM, Pemberton OA, Boragine DM, Chen Y, Palzkill T. KPC-2 β-lactamase enables carbapenem antibiotic resistance through fast deacylation of the covalent intermediate. J Biol Chem. 2021;296:100155.

Micsonai A, Wien F, Kernya L, Lee YH, Goto Y, Réfrégiers M, et al. Accurate secondary structure prediction and fold recognition for circular dichroism spectroscopy. Proc Natl Acad Sci U S A. 2015;112:E3095–103.

Micsonai A, Wien F, Bulyáki É, Kun J, Moussong É, Lee YH, et al. BeStSel: a web server for accurate protein secondary structure prediction and fold recognition from the circular dichroism spectra. Nucl Acids Res. 2018;46:W315–22.

Miller JH. Experiments in molecular genetics. Cold Spring Harbor, NY: Cold Spring Harbor Laboratory; 1972.

Miller A, Dudek D, Potocki S, Czapor-Irzabek H, Kozlowski H, Rowinska-Zyrek M. Pneumococcal histidine triads – involved not only in Zn^{2+}, but also Ni^{2+} binding? Metallomics. 2018;10: 1631–7.

Minami S, Yotsuji A, Inoue M, Mitsuhashi S. Induction of β-lactamase by various β-lactam antibiotics in Enterobacter cloacae. Antimicrob Agents Chemother. 1980;18:382–5.

Minasov G, Wang X, Shoichet BK. An ultrahigh resolution structure of TEM-1 β-lactamase suggests a role for Glu166 as the general base in acylation. J Am Chem Soc. 2002;124: 5333–40.

Mitchell SM, Ullman JL, Teel AL, Watts RJ. pH and temperature effects on the hydrolysis of three β-lactam antibiotics: ampicillin, cefalotin and cefoxitin. Sci Total Environ. 2014;466–467: 547–55.

Möhler JS, Kolmar T, Synnatschke K, Hergert M, Wilson LA, Ramu S, et al. Enhancement of antibiotic-activity through complexation with metal ions – combined ITC, NMR, enzymatic and biological studies. J Inorg Biochem. 2017;167:134–41.

Naas T, Oueslati S, Bonnin RA, Dabos ML, Zavala A, Dortet L, et al. Beta-lactamase database (BLDB) – structure and function. J Enzyme Inhib Med Chem. 2017;32:917–9.

Nafaee ZH, Hunyadi-Gulyás É, Gyurcsik B. Temoneira-1 β-lactamase is not a metalloenzyme, but its native metal ion binding sites allow for purification by immobilized metal

ion affinity chromatography. Protein Expr Purif. 2023;201: 106169.

Nagshetty K, Shilpa BM, Patil SA, Shivannavar CT, Manjula NG. An overview of extended spectrum beta lactamases and metallo beta lactamases. Adv Microbiol. 2021;11:37–62.

Nägele E, Moritz R. Structure elucidation of degradation products of the antibiotic amoxicillin with ion trap MS(n) and accurate mass determination by ESI TOF. J Am Soc Mass Spectrom. 2005;16:1670–6.

Oka T, Hashizume K, Fujta H. Inhibition of peptidoglycan transpeptidase by beta-lactam antibiotics: structure–activity relationships. J Antibiotics. 1980;33:1357–62.

Orabi AS. Physicochemical properties of ampicillin and amoxicillin as biologically active ligands with some alkali earth, transition metal, and lanthanide ions in aqueous and mixed solvents at 20, 30, and 40°C. J Sol Chem. 2005;34:95–111.

Pavlić A, Gobin I, Begić G, Tota M, Abram M, Špalj S. The effect of nickel ions on the susceptibility of bacteria to ciprofloxacin and ampicillin. Folia Microbiol (Praha). 2022;67:649–57.

Palzkill T. Structural and mechanistic basis for extended-spectrum drug-resistance mutations in altering the specificity of TEM, CTX-M, and KPC β-lactamases. Front Mol Biosci. 2018;5:16.

Peintler G, Nagypál I, Jancsó A, Epstein IR, Kustin K. Extracting experimental information from large matrixes. 1. A new algorithm for the application of matrix rank analysis. J Phys Chem. 1997;A101:8013–20.

Peintler G. ZiTa(1989–2012)/ChemMech(2013–2022), a comprehensive program package for fitting parameters of chemical reaction mechanisms, versions 2.1-5.99. Szeged, Hungary: Department of Physical Chemistry, University of Szeged; 1989–2022.

Perez-Garcia P, Kobus S, Gertzen CGW, Hoeppner A, Holzscheck N, Strunk CH, et al. A promiscuous ancestral enzyme's structure unveils protein variable regions of the highly diverse metallo-β-lactamase family. Commun Biol. 2021;4:132.

Potocki S, Delgado P, Dudek D, Janicka-Klos A, Kozlowski H, Rowinska-Zyrek M. Pneumococcal HxxHxH triad-copper (II) interactions—how important is the 'x'? Inorg Chim Acta. 2019;488:255–9.

Punekar NS. ES complex and pre-steady-state kinetics in ENZYMES: catalysis, kinetics and mechanisms. Singapore: Springer; 2018.

Pyreu DF, Ryzhakov AM, Kozlovskii EV, Gruzdev MS, Kumeev RS. Mixed-ligand complex formation of mercury (II) ethylenediaminetetraacetate with cysteine and methionine in aqueous solution. Inorg Chim Acta. 2011;371:53–8.

Rašić-Mišić I, Miletić G, Mitić S, Mitić M, Pecev-Marinković E. A simple method for the ampicillin determination in pharmaceuticals and human urine. Chem Pharm Bull (Tokyo). 2013;61:913–9.

Raza Siddiqui M, Alothman ZA, Mohammad WS. Ultraperformance liquid chromatography-mass spectrometric method for determination of ampicillin and characterization of its forced degradation products. J Chromatogr Sci. 2014;52:1273–80.

Remelli M, Brasili D, Guerrini R, Pontecchiani F, Potocki S, Rowinska-Zyrek M, et al. Zn(II) and Ni(II) complexes with poly-histidyl peptides derived from a snake venom. Inorg Chim Acta. 2018;472:149–56.

Robinson-Fuentes VA, Jefferies TM, Branch SK. Degradation pathways of ampicillin in alkaline solutions. J Pharm Pharmacol. 1997;49:843–51.

Rubino JT, Riggs-Gelasco P, Franz KJ. Methionine motifs of copper transport proteins provide general and flexible thioether-only binding sites for Cu(I) and Ag(I). J Biol Inorg Chem. 2010;15: 1033–49.

Salverda MLM, de Visser JAGM, Barlow M. Natural evolution of TEM-1 β-lactamase: experimental reconstructionand clinical relevance. FEMS Microbiol Rev. 2010;34:1015–36.

Samuni A. A direct spectrophotometric assay and determination of Michaelis constants for the β-lactamase reaction. Anal Biochem. 1975;63:17–26.

Scully CCG, Jensen P, Rutledge PJ. Mercury binding by ferrocenoyl peptides with sulfur-containing side chains: electrochemical, spectroscopic and structural studies. J Organomet Chem. 2008; 693:2869–76.

Sideraki V, Huang W, Palzkill T, Gilbert HF. A secondary drug resistance mutation of TEM-1 β-lactamase that suppresses misfolding and aggregation. Proc Natl Acad Sci U S A. 2001;98: 283–8.

Song WJ, Tezcan FA. A designed supramolecular protein assembly with in vivo enzymatic activity. Science. 2014;346:1525–8.

Sóvágó I, Petőcz G. Studies on transition-metal-peptide complexes. Part 13. Copper(II) and nickel(II) complexes of amino acids and peptides containing a thioether group. J Chem Soc Dalton Trans. 1987;(7):1717–20.

Stec B, Holtz KM, Wojciechowski CL, Kantrowitz ER. Structure of the wild-type TEM-1 β-lactamase at 1.55Å and the mutant enzyme Ser70Ala at 2.1Å suggest the mode of noncovalent catalysis for the mutant enzyme. Acta Crystallogr. 2005;D61: 1072–9.

Stiffler MA, Hekstra DR, Ranganathan R. Evolvability as a function of purifying selection in TEM-1 β-lactamase. Cell. 2015;160: 882–92.

Stojanoski V, Chow D, Hu L, Sankaran B, Gilbert HF, Prasad BVV, et al. A triple mutant in the Ω-loop of TEM-1 β-lactamase changes the substrate profile via a large conformational change and an altered general base for catalysis. J Biol Chem. 2015; 290:10382–94.

Stratton A, Ericksen M, Harris TV, Symmonds N, Silverstein TP. Mercury(II) binds to both of chymotrypsin's histidines, causing inhibition followed by irreversible denaturation/aggregation. Protein Sci. 2017;26:292–305.

Strynadka NC, Adachi H, Jensen SE, Johns K, Sielecki A, Betzel C, et al. Molecular structure of the acylenzyme intermediate in beta-lactam hydrolysis at 1.7 Å resolution. Nature. 1992;359: 700–5.

Studier FW, Rosenberg AH, Dunn JJ, Dubendorff JW. Use of T7 RNA polymerase to direct expression of cloned genes. Methods Enzymol. 1990;185:60–89.

Sun M, Wang Y, Zhang Q, Xia Y, Ge W, Guo D. Prediction of reversible disulfide based on features from local structural signatures. BMC Genomics. 2017;18:279.

Sy NV, Harada K, Asayama M, Warisaya M, Dung LH, Sumimura Y, et al. Residues of 2-hydroxy-3-phenylpyrazine, a degradation product of some β-lactam antibiotics, in environmental water in Vietnam. Chemosphere. 2017;172:355–62.

Tooke CL, Hinchliffe P, Bragginton EC, Colenso CK, Hirvonen VHA, Takebayashi Y, et al. β-Lactamases and β-lactamase inhibitors in the 21st century. J Mol Biol. 2019;431:3472–500.

Yang J, Naik N, Patel JS, Wylie CS, Gu W, Huang J, et al. Predicting the viability of beta-lactamase: how folding and binding free

energies correlate with beta-lactamase fitness. PLoS One. 2020; 15:e0233509.

Yang M-H, Lohani CR, Cho H, Lee K-H. A methionine-based turn-on chemical sensor for selectively monitoring Hg^{2+} ions in 100% aqueous solution. Org Biomol Chem. 2011;9:2350–6.

Vats P, Kaur UJ, Rishi P. Heavy metal-induced selection and proliferation of antibiotic resistance: a review. J Appl Microbiol. 2022;132:4058–76.

Wales AD, Davies RH. Co-selection of resistance to antibiotics, biocides and heavy metals, and its relevance to foodborne pathogens. Antibiotics (Basel). 2015;4:567–604.

Waley SG. A spectrophotometric assay of β-lactamase action on penicillins. Biochem J. 1974;139:789–90.

Wang X, Minasov G, Blázquez J, Caselli E, Prati F, Shoichet BK. Recognition and resistance in TEM β-lactamase. Biochemistry. 2003;42:8434–44.

Wilamowski M, Sherrell DA, Kim Y, Lavens A, Henning RW, Lazarski K, et al. Time-resolved β-lactam cleavage by L1 metallo-β-lactamase. Nat Commun. 2022;13:7379.

Wu C, Lin C, Zhu X, Liu H, Zhou W, Lu J, et al. The β-lactamase gene profile and a plasmid-carrying multiple heavy metal resistance genes of Enterobacter cloacae. Int. J Genomics. 2018; 2018:4989602–12.

Wuerz TC, Kassim SS, Atkins KE. Acquisition of extended-spectrum beta-lactamase-producing Enterobacteriaceae (ESBL-PE) carriage after exposure to systemic antimicrobials during travel: systematic review and meta-analysis. Travel Med Infect Dis. 2020;37:101823.

Zaworotko MJ, Hammud HH, Abbas I, Kravtsov VC, Masoud MS. Ampicillin acidity and formation constants with some metals and their thermodynamic parameters in different media. Crystal structures of two polymorphs isolated from the reaction of ampicillin with copper(II). J Coord Chem. 2006;59:65–84.

Zimmerman MI, Hart KM, Sibbald CA, Frederick TE, Jimah JR, Knoverek CR, et al. Prediction of new stabilizing mutations based on mechanistic insights from Markov state models. ACS Cent Sci. 2017;3:1311–21.

SUPPORTING INFORMATION

Additional supporting information can be found online in the Supporting Information section at the end of this article.

How to cite this article: Nafaee ZH, Egyed V, Jancsó A, Tóth A, Gerami AM, Dang TT, et al. Revisiting the hydrolysis of ampicillin catalyzed by Temoneira-1 β-lactamase, and the effect of Ni(II), Cd(II) and Hg(II). Protein Science. 2023;32(12): e4809. https://doi.org/10.1002/pro.4809